

ผลของการบำบัดเบื้องต้นด้วยน้ำต่อตัวเร่งปฏิกิริยาประเภทอะลูมินา  
ในปฏิกิริยาดีไฮเดรชันของเมทานอล

นายกฤษณ์ เลิศเจียมรัตน์

ศูนย์วิจัยทรัพยากร

วิทยานิพนธ์นี้เป็นส่วนหนึ่งของการศึกษาตามหลักสูตรปริญญาวิศวกรรมศาสตรมหาบัณฑิต

สาขาวิชาวิศวกรรมเคมี ภาควิชาวิศวกรรมเคมี

คณะวิศวกรรมศาสตร์ จุฬาลงกรณ์มหาวิทยาลัย

ปีการศึกษา 2552

ลิขสิทธิ์ของจุฬาลงกรณ์มหาวิทยาลัย

EFFECT OF WATER PRETREATMENT ON ALUMINA-BASED CATALYSTS IN  
METHANOL DEHYDRATION



Mr. Krit Lertjiamratn

A Thesis Submitted in Partial Fulfillment of the Requirements  
for the Degree of Master of Engineering Program in Chemical Engineering

Department of Chemical Engineering

Faculty of Engineering

Chulalongkorn University

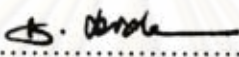
Academic Year 2009

Copyright of Chulalongkorn University

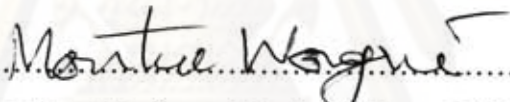
Thesis Title            EFFECT OF WATER PRETREATMENT ON ALUMINA-  
                                      BASED CATALYSTS IN METHANOL DEHYDRATION  
By                             Mr. Krit Lertjiamratn  
Field of Study            Chemical Engineering  
Thesis Advisor            Assistant Professor Joongjai Panpranot, Ph.D.

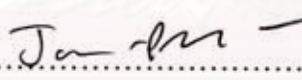
---


Accepted by the Faculty of Engineering, Chulalongkorn University in Partial  
Fulfillment of the Requirements for the Master's Degree


  
..... Dean of the Faculty of Engineering  
(Associate Professor Boonsom Lerthirunwong, Dr. Ing.)

THESIS COMMITTEE

  
..... Chairman  
(Assistant Professor Montree Wongsri, D.Sc.)

  
..... Thesis Advisor  
(Assistant Professor Joongjai Panpranot, Ph.D.)

  
..... Examiner  
(Assistant Professor Bunjerd Jongsomjit, Ph.D.)

  
..... External Examiner  
(Assistant Professor Okorn Mekasuwandumrong, D.Eng.)

กฤษณ์ เลิศเจียมรัตน์: ผลของการบำบัดเบื้องต้นด้วยน้ำต่อตัวเร่งปฏิกิริยาประเภทอะลูมินา  
 ในปฏิกิริยาดีไฮเดรชันของเมทานอล (EFFECT OF WATER PRETREATMENT ON  
 ALUMINA-BASED CATALYSTS IN METHANOL DEHYDRATION) อ.ที่ปรึกษา  
 วิทยานิพนธ์หลัก: ผศ.ดร.จุงใจ ปิ่นประฉศ, 70 หน้า

งานวิจัยนี้ทำการสังเคราะห์แกมมาอะลูมินาและอะลูมิเนียมฟอสเฟตที่มีโครงสร้างแบบ  
 อัญฐานเพื่อทดสอบในปฏิกิริยาดีไฮเดรชันของเมทานอลในช่วงอุณหภูมิการทำปฏิกิริยา 150 ถึง  
 300 องศาเซลเซียส ทั้งอะลูมินาและอะลูมิเนียมฟอสเฟตแสดงค่าความว่องไวในปฏิกิริยาสูงขึ้น เมื่อ  
 เปลี่ยนเส้นทางการทดสอบปฏิกิริยาจากการเพิ่มอุณหภูมิปฏิกิริยาทีละขั้น (150>200>250>300) เป็น  
 ลดลงทีละขั้น (300>250>200>150) เมื่อศึกษาผลของน้ำที่เป็นผลิตภัณฑ์ของปฏิกิริยา โดยการบำบัด  
 เบื้องต้นด้วยน้ำต่อคุณสมบัติในการเร่งปฏิกิริยาของอะลูมิเนียมฟอสเฟต จากการวิเคราะห์ด้วย  
 เทคนิค FT-IR และ FT-Raman พบว่าการบำบัดด้วยน้ำทำให้เกิดหมู่ฟังก์ชันไฮดรอกซิลขึ้นบนหมู่  
 ฟอสเฟต ซึ่งเป็นหนึ่งสารมัธยันต์สำหรับการเกิดปฏิกิริยาดีไฮเดรชันของเมทานอล การโคเรตด้วย  
 เอมีนพบว่าตัวเร่งปฏิกิริยาที่ผ่านการบำบัดเบื้องต้นด้วยน้ำมีปริมาณและความแรงของกรดเพิ่มขึ้น  
 จากการทดลองพบว่าช่วงอุณหภูมิที่เหมาะสมในการบำบัดเบื้องต้นของอะลูมิเนียมฟอสเฟตด้วยน้ำ  
 คือ ระหว่าง 200 ถึง 250 องศาเซลเซียส โดยมีโมลของน้ำเท่ากับร้อยละ 10 และเวลาที่ใช้ในการ  
 บำบัดเท่ากับ 15 นาที ในทางตรงกันข้าม การบำบัดด้วยอุณหภูมิที่ 100 องศาเซลเซียส ส่งผลให้เกิด  
 การปกคลุมของน้ำบนพื้นผิวของตัวเร่งปฏิกิริยาจากการดูดซับแบบกายภาพ ทำให้เมทานอลเกิดการ  
 ดูดซับบนพื้นผิวของตัวเร่งปฏิกิริยาได้ลดลงและทำให้ความว่องไวในปฏิกิริยาตกลง

ศูนย์วิทยทรัพยากร

จุฬาลงกรณ์มหาวิทยาลัย

ภาควิชา.....วิศวกรรมเคมี..... ลายมือชื่อนิสิต.....กฤษณ์ เลิศเจียมรัตน์.....  
 สาขาวิชา.....วิศวกรรมเคมี..... ลายมือชื่อ อ.ที่ปรึกษาวิทยานิพนธ์หลัก.....ผศ.ดร.จุงใจ.....  
 ปีการศึกษา.....2552.....

##50702103: MAJOR CHEMICAL ENGINEERING

KEYWORDS: AMORPHOUS ALUMINIUM PHOSPHATE/ GAMMA ALUMINA/  
METHANOL DEHYDRATION/ DIMETHYL ETHER/ WATER PRETREATMENT

KRIT LERTJIAMRATN: EFFECT OF WATER PRETREATMENT ON  
ALUMINA-BASED CTALYSTS IN METHANOL DEHYDRATION.  
THESIS ADVISOR: ASST. PROF. JOONGJAI PANPRANOT, Ph.D., 70 pp.

In this study,  $\gamma$ -Al<sub>2</sub>O<sub>3</sub> and amorphous AlPO<sub>4</sub> were synthesized and tested in methanol dehydration reaction. Both  $\gamma$ -Al<sub>2</sub>O<sub>3</sub> and AlPO<sub>4</sub> catalysts showed increasing of activity when temperature direction during reaction test changed from step-up (150>200>250>300) to step-down (300>250>200>150). The effect of the presence of water product was studied by pretreatment of AlPO<sub>4</sub> catalyst with water various conditions. FT-IR and FT-Raman results indicated formation of P-OH group on the pretreated catalysts, which was one of intermediate for methanol dehydration. Amine titration also showed increasing of both strength and amount of acid sites on surface of the treated catalysts. The appropriate temperature on AlPO<sub>4</sub> catalyst was determined to be 200-250°C for 10% mol of water in 5,300 h<sup>-1</sup> GHSV for 15 minutes. On the other hand, the presence of water at 100°C pretreatment became AlPO<sub>4</sub> poison which indicated by TGA and FT-Raman that physisorbed water could block the adsorption of methanol on catalyst active sites instead.



ศูนย์วิทยทรัพยากร

จุฬาลงกรณ์มหาวิทยาลัย

Department:....Chemical Engineering... Student's Signature: Krit Lertjiamratn.....

Field of Study:....Chemical Engineering... Advisor's Signature: J.P.N.....

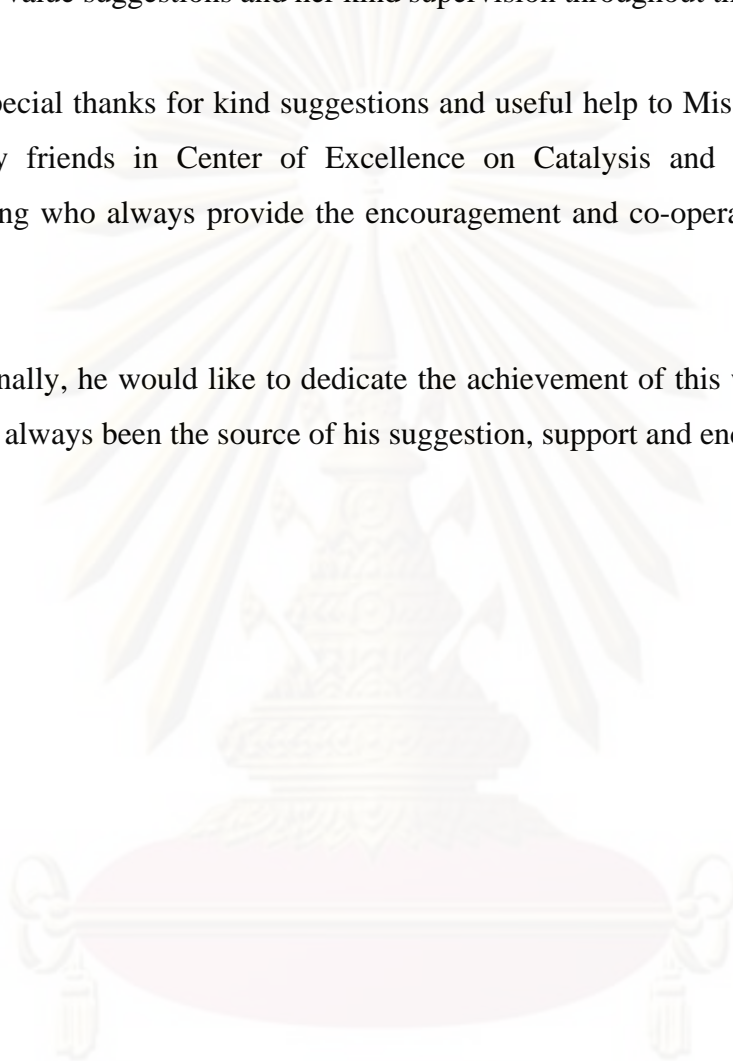
Academic Year:....2009.....

## ACKNOWLEDGEMENTS

The author would like to express his greatest gratitude and appreciation to his advisor, Assistant Professor Dr. Joongjai Panpranot for her invaluable guidance, providing value suggestions and her kind supervision throughout this study.

Special thanks for kind suggestions and useful help to Miss Jutharat Khom-in and many friends in Center of Excellence on Catalysis and Catalytic Reaction Engineering who always provide the encouragement and co-operate along the thesis study.

Finally, he would like to dedicate the achievement of this work to his parents who have always been the source of his suggestion, support and encouragement.



ศูนย์วิจัยทรัพยากร  
จุฬาลงกรณ์มหาวิทยาลัย

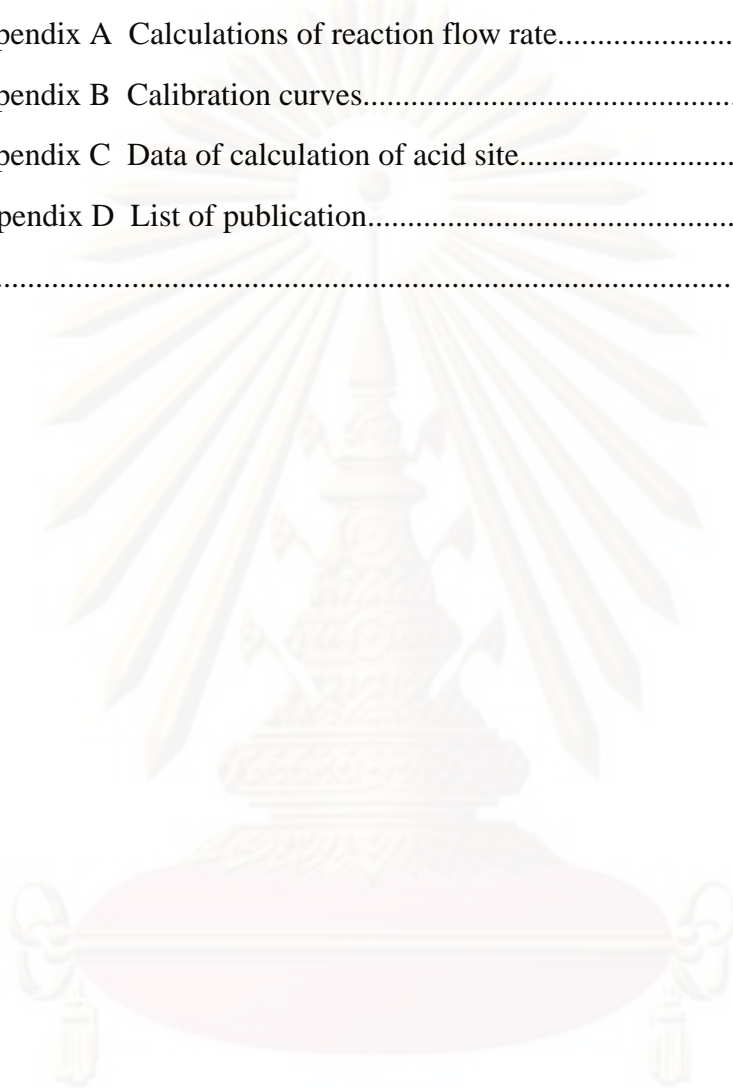
# CONTENTS

	<b>Page</b>
<b>ABSTRACT (THAI)</b> .....	iv
<b>ABSTRACT (ENGLISH)</b> .....	v
<b>ACKNOWLEDGMENTS</b> .....	vi
<b>CONTENTS</b> .....	vii
<b>LIST OF TABLES</b> .....	xi
<b>LIST OF FIGURES</b> .....	xii
<b>CHAPTER</b>	
<b>I INTRODUCTION</b> .....	1
<b>II LITERATURE REVIEWS</b> .....	3
2.1 Catalysts for methanol dehydration.....	3
2.2 Effect of water in methanol dehydration.....	8
2.3 Characterization and analysis.....	10
<b>III THEORY</b> .....	11
3.1 Dimethyl Ether: DME.....	11
3.2 Using of Dimethyl Ether.....	11
3.2.1 Household fuel.....	11
3.2.2 Transformation fuel.....	12
3.2.3 Fuel Cell .....	13
3.3 Effect of dimethyl ether on environment.....	14
3.4 Dimethyl ether Synthesis.....	15
3.4.1 Dimethyl ether synthesis from synthesis gas .....	15
3.4.2 Direct dimethyl ether synthesis from methanol .....	17
3.5 The Alumina.....	18
3.5.1 Properties of alumina.....	18
3.5.2 Properties of $\gamma$ - Al <sub>2</sub> O <sub>3</sub> .....	18
3.6 Aluminum Phosphate.....	22
<b>IV EXPERIMENTAL</b> .....	24
4.1 Catalyst preparation.....	24

4.1.1 Preparation of aluminum phosphate catalyst by precipitation method.....	24
4.1.2 Preparation of gamma alumina catalyst by solvothermal method .....	25
4.2 Catalyst characterization.....	28
4.2.1 X-Ray Diffraction pattern (XRD).....	28
4.2.2 Nitrogen physisorption.....	28
4.2.3 NH <sub>3</sub> Temperature Programmed Desorption (NH <sub>3</sub> -TPD).....	28
4.2.4 Thermogravimetric and differential thermal analysis (TG-DTA).....	29
4.2.5 Fourier transform infrared (FT-IR).....	29
4.2.6 Fourier transform Raman (FT-Raman).....	29
4.2.7 Amine titration using Hammett indicators.....	29
4.3 Reaction study in dehydration of methanol.....	31
4.3.1 Chemical and Reagents.....	31
4.3.2 Instrument and Apparatus.....	32
<b>V RESULTS AND DISCUSSION.....</b>	<b>35</b>
5.1 Characterization of fresh catalysts.....	35
5.1.1 X-ray Diffraction (XRD).....	35
5.1.2 Nitrogen physisorption.....	36
5.1.3 Ammonia Temperature Programmed Desorption (NH <sub>3</sub> -TPD).....	37
5.2 Reaction Study.....	38
5.2.1 Step-up and step-down temperature reaction test.....	38
5.2.2 Water pretreatment of AlPO <sub>4</sub> .....	41
5.3 Characterization of treated catalysts.....	44
5.3.1 Thermogravimetric analysis (TGA).....	44
5.3.2 Fourier transform Infrared (FT-IR).....	45
5.3.3 Fourier transform Raman (FT-Raman).....	50
5.3.4 Catalyst active site.....	53
<b>VI CONCLUSIONS AND RECOMMENDATIONS.....</b>	<b>56</b>



6.1 Conclusions.....	56
6.2 Recommendations.....	56
<b>REFERENCES</b> .....	58
<b>APPENDICES</b> .....	61
Appendix A Calculations of reaction flow rate.....	62
Appendix B Calibration curves.....	64
Appendix C Data of calculation of acid site.....	67
Appendix D List of publication.....	69
<b>VITA</b> .....	70



ศูนย์วิจัยทรัพยากร  
จุฬาลงกรณ์มหาวิทยาลัย



ต้นฉบับไม่มีหน้านี้  
NO THIS PAGE IN ORIGINAL

ศูนย์วิทยทรัพยากร  
จุฬาลงกรณ์มหาวิทยาลัย

## LIST OF TABLES

<b>TABLE</b>	<b>Page</b>
3.1 Physical properties of dimethyl ether and other fuel.....	12
3.2 Global warming potential properties of DME and other organic compound.....	14
4.1 Basic indicators used for the measurement of acid strength.....	31
4.3 Operating condition gas chromatograph for methanol dehydration reaction.....	34
5.1 Physical properties of amorphous $\text{AlPO}_4$ , synthesis and commercial $\text{Al}_2\text{O}_3$ .....	36
5.2 Acidity of amorphous $\text{AlPO}_4$ , synthesis and commercial $\text{Al}_2\text{O}_3$ .....	37
5.3 Amount of P-OH group of treated $\text{AlPO}_4$ from result of FT-IR and FT-Raman calculated by semi-quantity analysis method	52
5.4 Distribution of the acidic strength with the amount of acid of treated and non- treated $\text{AlPO}_4$ in different range of Hammett indicators	53


  
 ศูนย์วิจัยทรัพยากร  
 จุฬาลงกรณ์มหาวิทยาลัย

## LIST OF FIGURES

<b>FIGURE</b>	<b>Page</b>
3.1 Comparing of DME and other fuel in hydrogen production of fuel cell.....	14
3.2 Schematic of DME production processes.....	15
3.3 Equilibrium conversions of synthesis gas at 260°C and 5 MPa.....	16
3.4 Empirical reaction series of methanol reforming.....	18
3.5 Desorption of water from alumina surface.....	19
3.6 Lewis acid and Lewis basic sites on alumina.....	20
3.7 Assignment of the OH stretchings of transitional aluminas, following Busca et al., based on the comparison with the spectra of nondefective and partially defective spinel aluminates and ferrites. The square represents a vacancy in a normally occupied position of stoichiometric spinels.....	21
4.1 Autoclave reactor.....	26
4.2 Diagram of the reaction equipment for the synthesis of catalyst.....	27
4.3 A schematic of methanol dehydration system.....	32
5.1 XRD patterns of amorphous AlPO <sub>4</sub> , synthesis and commercial Al <sub>2</sub> O <sub>3</sub> in gamma phase.....	36
5.2 NH <sub>3</sub> -TPD Profiles of amorphous AlPO <sub>4</sub> , commercial $\gamma$ -Al <sub>2</sub> O <sub>3</sub> and synthetic solvothermal $\gamma$ -Al <sub>2</sub> O <sub>3</sub> catalysts.....	38
5.3 Methanol conversion profile of step-up reaction temperature (0.2 g catalyst, GHSV=5,300 h <sup>-1</sup> ).....	39
5.4 Methanol conversion profile of step-down reaction temperature (0.2 g catalyst, GHSV=5,300 h <sup>-1</sup> ).....	40
5.5 Effect of water pretreatment temperature of treated and non-treated amorphous AlPO <sub>4</sub> (0.2 g catalyst, GHSV=5,300 h <sup>-1</sup> , 10% mol water 15 minute pretreatment).....	42
5.6 Effect of the amount of water pretreatment of amorphous AlPO <sub>4</sub> (0.2 g catalyst, GHSV=5,300 h <sup>-1</sup> , 10% mol water 15 minute pretreatment).....	43
5.7 TGA profile of treated and non-treated amorphous AlPO <sub>4</sub> from 50-650°C....	44
5.8 FTIR adsorption bands from wavelength of 400-1800 cm <sup>-1</sup> of non-treated AlPO <sub>4</sub> and 100-300°C water pretreatment.....	46

<b>FIGURE</b>	<b>Page</b>
5.9 FTIR adsorption bands from wavelength of 2500-4000 $\text{cm}^{-1}$ of non-treated $\text{AlPO}_4$ and 100-300°C water pretreatment $\text{AlPO}_4$ .....	47
5.10 De-convolution FT-IR spectra of hydroxyl group of non-treated $\text{AlPO}_4$ .....	48
5.11 De-convolution FT-IR spectra of hydroxyl group of water pretreatment 100°C $\text{AlPO}_4$ , 10% mol water for 15 minute.....	48
5.12 De-convolution FT-IR spectra of hydroxyl group of water pretreatment 200°C $\text{AlPO}_4$ , 10% mol water for 15 minute.....	49
5.13 De-convolution FT-IR spectra of hydroxyl group of water pretreatment 250°C $\text{AlPO}_4$ , 10% mol water for 15 minute.....	49
5.14 De-convolution FT-IR spectra of hydroxyl group of water pretreatment 300°C $\text{AlPO}_4$ , 10% mol water for 15 minute.....	50
5.15 FT-Raman spectra bands at Raman shift of 900-1500 $\text{cm}^{-1}$ of non-treated $\text{AlPO}_4$ and 100-300 °C pretreatment $\text{AlPO}_4$ .....	51
B1 The calibration curve of methanol from Porapak-Q.....	64
B2 The calibration curve of water from Porapak-Q.....	65
B3 The calibration curve of DME from Porapak-Q.....	65
B4 The calibration curve of methanol from Porapak-N.....	65
B5 The calibration curve of water from Porapak-N.....	66
B6 The calibration curve of water from Porapak-N.....	66
B7 The calibration curve of carbon monoxide from Porapak-N.....	66

ศูนย์วิจัยทรัพยากร

จุฬาลงกรณ์มหาวิทยาลัย

# CHAPTER I

## INTRODUCTION

In present, world's energy consumption is continuously increasing together with industrial and transportation expansion. World most important and useful energy reservoirs are crude oil and natural gas. In 1985, there was more than 54 million barrel per day of oil consumption; it increases to 85 million barrel per day in 2005. There is anticipating following by world economic growth and the truth that oil is circumscription energy and will be used up in the future oil consumption will be 75% increase more in 2010 and its price will continuously increase [Semelsberger et al. 2006]. For these reasons, research and development of alternative energy for oil replacement has received much attention continuously in order to find the most suitable alternative energy in the future.

Dimethyl ether (DME) is one of the promising alternative fuels due to their huge reservoir and easy production. Dimethyl ether can be used to substitute for liquefied petroleum gas (LPG) and diesel engine because of their similar properties of LPG and high cetane number. Dimethyl ether can be produced from either synthesis gas or methanol. In this study, production of only dimethyl ether from methanol dehydration is focused.

The most acceptable catalyst for methanol dehydration is gamma alumina ( $\gamma$ - $\text{Al}_2\text{O}_3$ ) due to its suitable acidity in this reaction but still there are studies in the way of modification of  $\gamma$ - $\text{Al}_2\text{O}_3$ . One of the very interesting catalysts is amorphous aluminum phosphate ( $\text{AlPO}_4$ ), modified gamma alumina with phosphate group, because of their ability to reduce coking and by-products. Moreover,  $\text{AlPO}_4$  give a promising property to resist water that occurs during methanol dehydration reaction. There are many studies reporting that water could be poison in this reaction. However, some studies report an opposite result that water could be help to increase activity of catalysts in dehydration reaction. One of reasonable hypotheses that is if there is water in reaction, Lewis acid sites could change to Brønsted acid sites which is stronger than Lewis one. This study is

aimed to investigate the effect of water during methanol dehydration over gamma alumina and aluminum phosphate catalysts.

The objectives of this research are to investigate catalytic behavior of  $\gamma$ -Al<sub>2</sub>O<sub>3</sub> and AlPO<sub>4</sub> catalysts in dehydration of methanol to dimethyl ether and the effect of water pretreatment on AlPO<sub>4</sub> catalyst.

#### Research scope

1. Synthesis of  $\gamma$ -Al<sub>2</sub>O<sub>3</sub> by solvothermal method
2. Synthesis of AlPO<sub>4</sub> by precipitation method
3. Study the catalyst pretreatment with 5% to 20% mol water vapor, pretreatment temperature 100°C to 300°C and pretreatment time
4. Catalyst activity test in methanol dehydration at 150-300°C and atmosphere pressure
5. Catalyst characterization using various techniques such as X-ray diffraction (XRD), N<sub>2</sub> physisorption, Ammonia temperature programmed desorption (NH<sub>3</sub>-TPD), Thermogravimetric and differential thermal analysis (TG-DTA), Fourier transform infrared (FT-IR), Fourier transform Raman (FT-Raman) and Amine titration using Hammett indicators.

The present thesis is divided into 6 chapters as follows:

- |             |   |
|-------------|---|
| Chapter I   | Background and introduction   |
| Chapter II  | Reviews of the literature.  |
| Chapter III | Basic theory about dimethyl ether (DME), synthesis of dimethyl ether (DME) over $\gamma$ -Al <sub>2</sub> O <sub>3</sub> and AlPO <sub>4</sub> catalysts. |
| Chapter IV  | Experimental  |
| Chapter V   | Results and discussions   |
| Chapter VI  | Conclusions and Recommendations   |

## CHAPTER II

### LITERATURE REVIEW

#### 2.1 Catalysts for methanol dehydration

It is known that in dehydration of hydrocarbon reaction acidity is needed to catalyze reaction. Many solid-acid substances are used as catalyst such as zeolite and alumina. Methanol dehydration reaction also needs acid catalyst but medium acidity is necessary if high methanol conversion and selectivity of dimethyl ether (DME) are desired. Many researchers have established knowledge about suitable acidity in methanol dehydration to dimethyl ether. These reports are very useful to develop better catalysts in the future.

Since 1997, Xu et al. [Xu et al. 1997] studied the catalytic conversion of methanol to dimethyl ether (DME) over a series of solid-acid catalysts, such as  $\gamma$ -Al<sub>2</sub>O<sub>3</sub>, H-ZSM-5, amorphous silica-alumina, as well as titania modified zirconia. They were found that all the catalysts are active and selective for DME formation. In 2002, Jun et al. [Jun et al. 2002] studied the conversion of methanol to dimethyl ether (DME) over  $\gamma$ -Al<sub>2</sub>O<sub>3</sub> and modified  $\gamma$ -Al<sub>2</sub>O<sub>3</sub> with SiO<sub>2</sub>, ZrO<sub>2</sub>, and B<sub>2</sub>O<sub>3</sub> which were synthesized by impregnation method. They were found that the order of the activity at 5 wt% loaded of all catalyst was SiO<sub>2</sub>/ $\gamma$ -Al<sub>2</sub>O<sub>3</sub> > ZrO<sub>2</sub>/ $\gamma$ -Al<sub>2</sub>O<sub>3</sub>  $\approx$   $\gamma$ -Al<sub>2</sub>O<sub>3</sub> > B<sub>2</sub>O<sub>3</sub>/ $\gamma$ -Al<sub>2</sub>O<sub>3</sub> because SiO<sub>2</sub>/ $\gamma$ -Al<sub>2</sub>O<sub>3</sub> had the highest acidity and became rather hydrophobic resulting in the decrease of sorption capacity of water. Then, vary wt% loading of SiO<sub>2</sub>/ $\gamma$ -Al<sub>2</sub>O<sub>3</sub> was examined and found that the  $\gamma$ -Al<sub>2</sub>O<sub>3</sub> modified with 1 wt% silica was more active and less deactivated by water.

In 2004, Duarte de Farias et al. [de Farias et al. 2004] evaluated Al<sub>2</sub>O<sub>3</sub>•B<sub>2</sub>O<sub>3</sub> catalysts which were synthesized by co-precipitation and impregnation methods applying two calcinations temperatures and boria loadings in methanol dehydration. Catalysts were



analyzed by IR spectroscopy of pyridine and CO<sub>2</sub> adsorption. Results showed that boron addition to alumina causes a decrease of the number of basic and Lewis acid sites on alumina surface. It could also be observed an enhancement in acid strength of Lewis sites for impregnated samples. These results showed that boron did not have any promoting effect in methanol dehydration.

Next, Jiang et al. [Jiang et al. 2004] investigated methanol dehydration to dimethyl ether (DME) over ZSM-5 zeolites. Although the catalytic activity was decreased with an increase in silica/alumina ratio, the DME selectivity increased. H-ZSM-5 and NaH-ZSM-5 zeolites were more active for conversion of methanol to DME. Na<sup>+</sup> ion-exchanged H-ZSM-5 (NaH-ZSM-5) showed higher DME selectivity than H-ZSM-5 due to eliminating of strong acid sites.

Then Vishwanathan et al. [Vishwanathan et al. 2004] studied a series of TiO<sub>2</sub>-ZrO<sub>2</sub> mixed oxides with varying molar ratio of TiO<sub>2</sub> to ZrO<sub>2</sub> which were prepared by the co-precipitation method. The catalytic activities were investigated for the vapor phase dehydration of methanol to dimethyl ether (DME) in a fixed-bed reactor under atmospheric pressure. The acid-base properties and CH<sub>3</sub>OH conversion activity are increasing with TiO<sub>2</sub> content and an optimum value is achieved for a molar ratio of Ti/Zr in the vicinity of 1/1. At lower reaction temperature (<300°C), the selectivity for DME is nearly 100%. TiO<sub>2</sub>-ZrO<sub>2</sub> catalysts show high stability against water during dehydration reaction.

And they [Vishwanathan et al. 2004] investigated a series of Na-modified H-ZSM-5 catalysts, with Na content varying from 0 to 80 mol%, which were prepared by an impregnation method tested for the dehydration of crude methanol (i.e. pure/anhydrous methanol containing 20 mol% of H<sub>2</sub>O) in a fixed-bed micro-reactor under normal atmospheric pressure. Though the unmodified H-ZSM-5 catalyst was more active and stable in the presence of water, the Na-modified H-ZSM-5 catalysts showed the optimum activity (CMeOH > 80%) and 100% selectivity for DME in a wide range of temperatures: 230–340°C. The catalysts were tested for the time-on-stream (TOS) and remained least

sensitive towards water for a total reaction period of 65 hours. The superior performance of Na-modified H-ZSM-5 catalyst is attributed mainly to the elimination of strong surface acid-sites by partial substitution of Na in H-ZSM-5, resulting in the prevention of coke and/or hydrocarbon formation.

Fu et al. [Fu et al. 2005] studied the nature, strength and number of surface acid sites of H-ZSM-5, steam de-aluminated H-Y zeolite (SDY),  $\gamma$ -Al<sub>2</sub>O<sub>3</sub>, and Ti(SO<sub>4</sub>)<sub>2</sub>/ $\gamma$ -Al<sub>2</sub>O<sub>3</sub> catalysts for dehydration of methanol to dimethyl ether (DME). The H-ZSM-5 and SDY possessed strong Brønsted acidity and exhibited high activity for conversion of methanol to DME at relatively low temperatures. Coke formation was serious over the two zeolite catalysts at 553 K. The dehydration of methanol to DME on  $\gamma$ -Al<sub>2</sub>O<sub>3</sub> was found to be low at the temperatures below 573 K though the DME selectivity is high. The modification of  $\gamma$ -Al<sub>2</sub>O<sub>3</sub> by Ti(SO<sub>4</sub>)<sub>2</sub> greatly enhanced the surface Brønsted acidity and also the reaction activity for the dehydration of methanol to DME. In addition, no detectable hydrocarbon by-products and coke were formed on the Ti(SO<sub>4</sub>)<sub>2</sub>/ $\gamma$ -Al<sub>2</sub>O<sub>3</sub> catalyst in the temperature range of 513–593 K. Thus, the Brønsted acid sites with suitable strength may be responsible for the effective conversion of methanol to DME with high stability. This study could be concluded that zeolites were not suitable in this reaction because of their highly acidity that caused coke formation on surface and deactivated the catalyst. Moreover, the appropriate amount of Brønsted acid sites is necessary for this reaction.

A number of studies follow the same trend, Fei et al. [Fei et al. 2006] examined synthesis of dimethyl ether (DME) via methanol dehydration over HY zeolite and Fe-, Co-, Ni-, Cr-, or Zr modified HY zeolite. Zr- and Ni-modified HY zeolite exhibited higher activity and stability for methanol dehydration, while Fe-, Co-, and Cr-modified HY zeolite deactivated quickly due to carbon deposition. Moreover, Kim et al. [Kim et al. 2006] studied the effect of  $\gamma$ -Al<sub>2</sub>O<sub>3</sub> as a binder on the catalytic performance of Na-modified ZSM-5 which was investigated by using the dehydration of methanol to dimethyl ether (DME). Though the addition of  $\gamma$ -Al<sub>2</sub>O<sub>3</sub> lowered the activity of NaHZSM-5, it broadened the operative temperature range (OTR), thereby resulting in more stable

catalysts. The ZSM-5 containing 70% of  $\gamma$ - $\text{Al}_2\text{O}_3$  was found to be an efficient catalyst, exhibiting quite high activity as well as wide OTR. This beneficial effect was ascribed to the adequate dilution of the strong acid sites of ZSM-5 in the  $\gamma$ - $\text{Al}_2\text{O}_3$  matrix.

Although,  $\gamma$ - $\text{Al}_2\text{O}_3$  seems to be suitable catalyst in methanol dehydration, there are studies on modification of  $\gamma$ - $\text{Al}_2\text{O}_3$  showing higher catalyst activity. Yaripour et al. [Yaripour et al. 2005] studied a series of solid-acid catalysts with different components contents which were prepared by co-precipitation (sol-gel) method comprised of  $\gamma$ - $\text{Al}_2\text{O}_3$  and modified  $\gamma$ - $\text{Al}_2\text{O}_3$  with silica. Dehydration of methanol to dimethyl ether (DME) on solid-acid catalysts was studied in a fixed bed flow reactor at a temperature of 300 °C under atmospheric pressure and a GHSV of 15,600  $\text{h}^{-1}$ . According to the experimental results, the pure  $\gamma$ - $\text{Al}_2\text{O}_3$  catalyst shown a good catalytic activity, but this sample undergoes a fairly rapid and irreversible deactivation. Silica-modified catalysts have shown better performance compared to the untreated  $\gamma$ - $\text{Al}_2\text{O}_3$ . It was found that surface areas and surface acidity increase with increasing in the silica loading for these aluminosilicate catalysts.

Khom-In et al. [Khom-In et al. 2008] studied  $\gamma$ - $\text{Al}_2\text{O}_3$ ,  $\chi$ - $\text{Al}_2\text{O}_3$  and mixed  $\gamma$ - and  $\chi$ -crystalline phases with various ratios as catalyst in methanol dehydration. They found  $\gamma$ - $\text{Al}_2\text{O}_3$  catalyst containing 20 wt% of  $\chi$ -phase which was synthesized by solvothermal method exhibited the highest DME yield. The  $\text{NH}_3$ -TPD and ion-exchange titration results revealed that the existence of 20 wt%  $\chi$ -phase in solvothermal synthesized  $\gamma$ - $\text{Al}_2\text{O}_3$  with synthesized by solvothermal method increased significantly both the density and the strength of surface acidity of alumina.

Furthermore, Yaripour et al. [Yaripour, Baghaei et al. 2005] also investigated silica-titania and modified  $\gamma$ - $\text{Al}_2\text{O}_3$  with phosphorus which were prepared by co-precipitation (sol-gel) method in dehydration of methanol to dimethyl ether (DME). Silica-titania catalysts exhibited low activity for DME synthesis. Phosphorus-modified catalysts showed better performance compared to the untreated  $\gamma$ - $\text{Al}_2\text{O}_3$ . It was found that surface areas increased with increasing in the molar ratio of aluminum-to-phosphorus

aluminum phosphate catalysts. Also, it was observed that the surface acidity of aluminum phosphate catalysts decreased with increasing molar ratio of Al/P at aluminum phosphate catalysts. The sample of non-stoichiometric aluminum phosphate (molar ratio of Al/P = 2) exhibited the best conversion without any by-product.

Modified alumina catalyst with phosphate or aluminum phosphate is very interesting because of their abilities to reduce the amounts of coking and by-products. However, aluminum phosphate is strongly dependent on the method of preparation, chemical composition (Al/P molar ratio), and activation temperature.

Aluminum phosphate has structure in both crystalline and amorphous structure. Kumar et al. [Kumar et al. 2006] studied activated of aluminum phosphate in methanol dehydration reaction. Co-precipitation and impregnation were chosen method as the preparation method of aluminum phosphate which had ratio of aluminum and phosphorus as 1:1. Aluminum nitrate ( $\text{Al}(\text{NO}_3)_3 \cdot 9\text{H}_2\text{O}$ ) was used as a aluminum precursor but in phosphate precursor, both ammonium hydrogenphosphate ( $(\text{NH}_4)_2\text{HPO}_4$ ) and phosphoric acid ( $\text{H}_3\text{PO}_4$ ) were chosen. The result has shown that all catalysts which were prepared by co-precipitation method had structure in amorphous structure. However, for impregnation method only catalyst that had phosphoric acid as phosphate precursor showed amorphous structure while the use of ammonium hydrogenphosphate gave crystalline phase catalyst. Reaction test result has shown that amorphous aluminum phosphate gave higher activity than crystalline one because of their significant different in acidity and surface area. At  $350^\circ\text{C}$ , amorphous aluminum phosphate from co-precipitation method gave rapid increase of conversion but decreasing in amorphous aluminum phosphate from impregnation method. Therefore, more experiment pointed that decreasing of activity due to changing in structure from amorphous to crystalline one. This study could be concluded that suitable phase of aluminum phosphate is amorphous structure.

## 2.2 Effect of water in methanol dehydration

The effect of water in methanol dehydration has been reported. It is shown that water is poison of catalyst in this reaction. Xu et al. [Xu et al. 1997] report that most of solid-acid catalyst deactivated during reaction when water was existed. They proposed that water would block active site and impede methanol from adsorption on active site.

Jun et al. [Jun et al. 2002] studied the effect of water on activity of  $\gamma\text{-Al}_2\text{O}_3$  in methanol dehydration by addition of 65 torr vapor pressure of water in substance. The result showed that activity of catalyst at temperature 523 K was significant decreased from 70% to 37% conversion of methanol after 40 hour of vapor stream. They pointed that water in reaction decreased activity of the catalyst because molecule of water adsorbed on active sites of catalyst. Although, Lewis acid sites could change to Brønsted acid if there was water in reaction but Brønsted acid sites of  $\gamma\text{-Al}_2\text{O}_3$  is very weak acid. Moreover, kinetic data confirm that increasing of activated energy of dimethyl ether synthesis is equal to the increasing of energy by added water that came from heat of adsorption of water (about 16 kcal/mol) when water covered most of surface of catalyst. In addition, water that exists in reaction would reverse equilibrium of reaction and decrease activity of methanol dehydration also.

However, there are some studies reported an opposite result that water in reaction could increase activity of catalyst instead of deactivate catalyst. One of the explanations is that Lewis acid sites could be changed to Brønsted acid sites and gave more activity to catalyst. Ramos et al. [Ramos et al. 2005] studied the role of Brønsted and Lewis acid sites in synthesis of DME and concluded that either Brønsted acid sites or Lewis acid–base pair sites are play a role in such reaction and, generally, the stronger the acid sites the more active the catalysts. However, it should be recalled that as far as Brønsted sites are involved, their strength and the reaction temperature should be controlled to avoid hydrocarbons formation. The mechanism based on Lewis acidity, on the other hand, requires an adjacent acid–base pair sites to provide the reaction between the adsorbed

alcohol molecule on an acidic site and an adsorbed alkoxide anion on a basic site. These interesting phenomena have been found on the catalysts with phosphate group.

András Ludmány et al. [Ludmany et al. 2004] studied physical and catalytic properties of amorphous titanium hydrogenphosphate ( $\text{Ti}(\text{HPO}_4)_2$ ) and proved that it could be an active catalyst in alcohol dehydration also; cyclohexanol, methanol and pentanol were chosen as substances. Main part of study focused on cyclohexanol dehydration, 100% conversion of cyclohexanol was reached at temperature of  $350^\circ\text{C}$  and the conversion was still the same even temperature was decreased to  $300^\circ\text{C}$ . Two further experiments were carried out to explain this interesting phenomenon. One titanium hydrogen phosphate was activated by argon atmosphere and another one in vapor pressure at  $280^\circ\text{C}$  before they were tested in cyclohexanol dehydration until 50% conversion at  $280^\circ\text{C}$  and step temperature down to  $250^\circ\text{C}$ . The first catalyst that activated with argon was almost ineffective but the second one was highly active in a short time. It could be concluded that water is a major cause of conversion increasing of alcohol dehydration reaction. From DTA results (differential thermal analysis) and TG (thermo gravimetric) of amorphous titanium hydrogenphosphate showed that catalyst has similar structure with crystalline alpha phase more than gamma phase of titanium hydrogenphosphate. Moreover, the literature data said that alpha phase of titanium hydrogenphosphate could be changed to gamma phase by heating in 10M of phosphoric acid and inter layer of titanium hydrogenphosphate were also increasing ( $7.6 \text{ \AA}$  and  $10.6 \text{ \AA}$  for alpha and gamma phase respectively) because of insertion of hydration water, This swollen molecule could bring some inserted alcohol in catalyst with water and give more activity of catalyst. The swollen catalyst with water and alcohol inside the layers retains its high activity until it loses the alcohol and water by evaporation.

In addition, Fu et al. [Fu, Hong et al. 2005] reported that when they regenerated coke form SDY zeolite after methanol dehydration reaction at 773 K for 2 hour, the activity of regenerated catalyst increase from 86.5% of fresh catalyst to 87.5% conversion of methanol at 503 K. Although, regeneration might recovered the activity completely,

clearly indicating that the de-activation was indeed due to the coking. But it could be an effect of water that increased activity of catalyst also.

### 2.3 Characterization and analysis

There are several studies of catalysts characterization and analysis of the reactant product. These reports are very useful and guideline for this works. Ng [Ng 2002] studied the effects of drying on catalyst activities in methanol dehydration. A feed gas mixture consisting of 10% methanol balanced in helium was introduced into the top bed reactor, which was maintained at the reaction. Gaseous methanol was introduced into the system via an evaporator-condenser system and the methanol containing gas stream was preheated and then trace heated to avoid condensation. At the downstream of the reactor, trace heating was also applied to avoid liquid products condensation. A small fraction of the reactor effluent was piped to a G.C. for on-line analysis. The catalytic activity was calculated based on  $\text{CH}_3\text{OH}$  conversion or  $\text{CH}_3\text{OCH}_3$  yield. Other compounds in the effluent stream ( $\text{CO}$ ,  $\text{CO}_2$ ,  $\text{H}_2\text{O}$ ,  $\text{CH}_3\text{OH}$  and  $\text{CH}_3\text{OCH}_3$ ) were analysed on-line with a Shimadzu 14B gas chromatograph with a TCD detector and a Porapak-Q column operating at  $110^\circ\text{C}$ .

## CHAPTER III

### THEORY

#### 3.1 Dimethyl Ether: DME

Dimethyl ether (DME;  $C_2H_6O$ ) is ether compound having molecular structure as  $CH_3-O-CH_3$ , may be known in other name such as Methoxymethane or Oxybismethane or Wood Ether. Dimethyl Ether is colorless gas at room temperature and ambient condition. In present, most of produced dimethyl ether are used as aero-propellant in spray bottle substitute of chlorofluorocarbons (CFCs) because of CFCs' potential as ozone destroyer in stratosphere atmosphere. Moreover, dimethyl ether is self-decompose gas in troposphere atmosphere and having less danger for human than CFCs.

Dimethyl ether can be called the "Clean Energy Media in the 21st Century" and expected to be regarded as new energy. Dimethyl ether has general physical properties resemble to LPG (LPG is consisted of propane and butane) such as boiling point flash point density vapor pressure and heat capacity. Moreover, dimethyl ether can be used instead of diesel due to their high cetane number property. Table 3.1 shows physical properties of dimethyl ether and other fuel.

#### 3.2 Using of Dimethyl Ether

##### 3.2.1 Household fuel

A number of under-development countries have still used either wood or charcoal as fuel for cooking that produce a lot of smoke and carbondioxide. As known as usual, major cause of air pollution and global warming are from carbondioxide therefore, liquid petroleum and propane are used substitute. However, there is study show that dimethyl ether could be used substitute also, because of properties of dimethyl ether are very similar to propane such as boiling point density and specific gravity as shown in table 3.1. Advantages of using dimethyl ether are storage and transportation because dimethyl



ether can easier to be compressed to liquid than liquid petroleum due to lower boiling point (-25 degree Celsius for dimethyl ether and -42.1 degree Celsius for liquid petroleum). Dimethyl ether can be compressed to liquid with 0.6 MPa at 25 degree Celsius which can directly use liquid petroleum compression factory to operate with lower operation energy.

**Table 3.1** Physical properties of dimethyl ether and other fuel. [Takashi et al. 2003]

Properties	DME	Propane	Methane	Methanol	Diesel
Molecular Structure	CH <sub>3</sub> OCH <sub>3</sub>	C <sub>3</sub> H <sub>8</sub>	CH <sub>4</sub>	CH <sub>3</sub> OH	-
Boiling Point (K)	247.9	231	111.5	337.6	370
Liquid Density at 293 K	0.67	0.49	-	0.79	0.84
Specific Gravity (versus air)	1.59	1.52	0.55	-	-
Vapor Pressure) atm) at 293 K	6.1	9.3	-	-	-
Flash Point) K)	623	777	905	743	-
Cetane Number	55-60	5	0	5	40-55
Net Calorific Value )10 <sup>6</sup> J/Nm <sup>3</sup> (	59.44	91.25	36	-	-
Net Calorific Value )J/kg)	28.9	46.46	50.23	21.1	41.86

### 3.2.2 Transformation fuel

Because of very similar physical properties of dimethyl ether and LPG, using of dimethyl ether substitute in LPG engine could be done nearly without engine and storage tank modification. Although, dimethyl ether give net calorific value 65 percent lower than propane (28.90 MJ/kg for dimethyl ether and 91.25 MJ/kg for propane) but dimethyl ether has 37 percent more density in liquid phase than propane because of its lower boiling point. Therefore, same volume of storage tank, dimethyl ether give 85 percent net

energy of propane with advantage in storage and transportation because of its boiling point that made dimethyl ether is easier to compress to liquid phase. [Takashi et al. 2003]

Moreover, dimethyl ether has high cetane number (55-60 for dimethyl ether and 40-55 for diesel) and can be used as a fuel in diesel engine also. Small size molecule of dimethyl ether and higher cetane number make a better ignition than diesel itself, with nearly complete ignition, there is no burning particles occur during ignition.

Another advantage of dimethyl ether is its ultraclean fuel property; there is no nitrogen and sulfur in molecule of dimethyl ether, there is no sulfur dioxide occurred and significant decrease among of nitrogen oxide by using dimethyl ether especially comparison with diesel, a large among of sulfur dioxide comes from their 250 ppm of sulfur in diesel. [Yataro et al. 2001]

These special properties of ultraclean fuel of dimethyl ether, decrease emission of small particle  $\text{NO}_x$  and  $\text{SO}_x$ , study and experiment of using dimethyl ether as a fuel in diesel engine in real transportation of JFE Company in Japan [JFE Holding Inc. 2001] and results are

1. Smokeless emission form engine because of there is no carbon-to-carbon bond in structure of dimethyl ether molecule.
2. Decreasing 20-30 percent of nitrogen oxide emission
3. Decreasing of ignition time and higher efficiency of engine
4. Operating without noise

### **3.2.3 Fuel Cell**

Another alternative energy is fuel cell. Fuel cell operates by changing chemical energy to electricity and heat. Fuel cell gives no emission because of using energy directly without fuel ignition. Main mechanism of fuel cell is chemical reaction of hydrogen and oxygen which give electricity and heat with water as an emission.

Fuel cell for vehicles usually use methane methanol and benzene as a hydrogen reservoir however, these substances need high temperature in reaction to give high conversion of hydrogen. Dimethyl ether can produce high among of hydrogen in low temperature with nearly efficiency of using methanol in figure 3.1

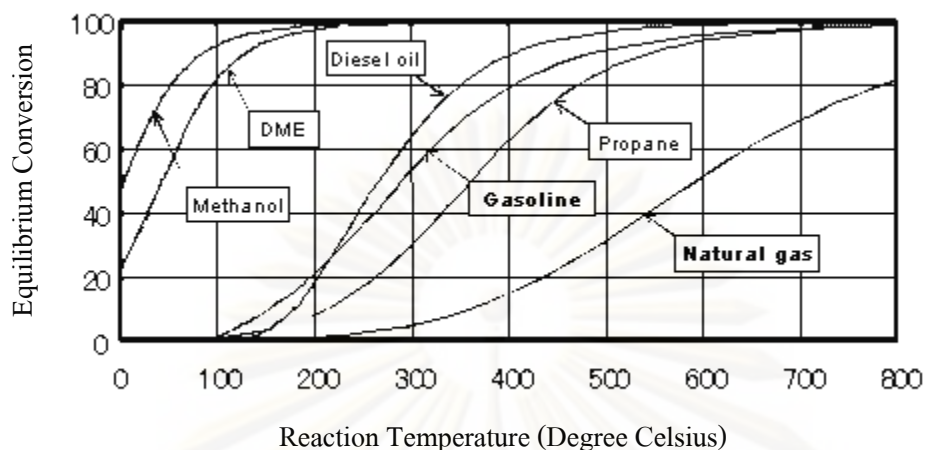


**Figure 3.1** Comparing of DME and other fuel in hydrogen production of fuel cell  
[JFE Holding Inc. 2001]

### 3.3 Effect of dimethyl ether on environment

Although, dimethyl ether is volatile hydrocarbon compound but there is neither poison nor cancer. Another significant effect is global warming potential of dimethyl ether as shown in table 3.2

**Table 3.2** Global warming potential properties of DME and other organic compound.  
[Yaripour et al. 2005]

Organic compound	Global warming potential property by years after emission.		
	20 years	30 years	500 years
Dimethyl Ether	1.2	0.3	0.1
Carbondioxide	1	1	1
Methane	56	21	6.5
Dinitrogenoxide	280	310	170

From table 3.2 dimethyl ether has global warming potential less than other global warming compound which base on carbondioxide potential. In first 20 years is 1.2 and decrease to 0.1 in 500 years, It's mean that dimethyl ether spend time to decay in

atmosphere less than other poison compound, such as carbondioxide that cannot be decay or having no decreasing in global warming potential in atmosphere even 500 years after emission. Moreover, compare to Dinitrogenoxide with 170 times global warming potential more than carbondioxide in 500 years with 0.1 times of Dimethyl Ether. This property can make sure than there will be no global warming problem form dimethyl ether emission [Semelsberger et al. 2006].

### 3.4 Dimethyl ether Synthesis

The DME production processes are an indirect synthetic method using the dehydration reaction of methanol and a direct synthetic method of producing DME from synthesis gas made from coal, biomass, natural gas and so on. At present, DME is usually made by the indirect method and technology development for the direct synthetic method is being implemented.

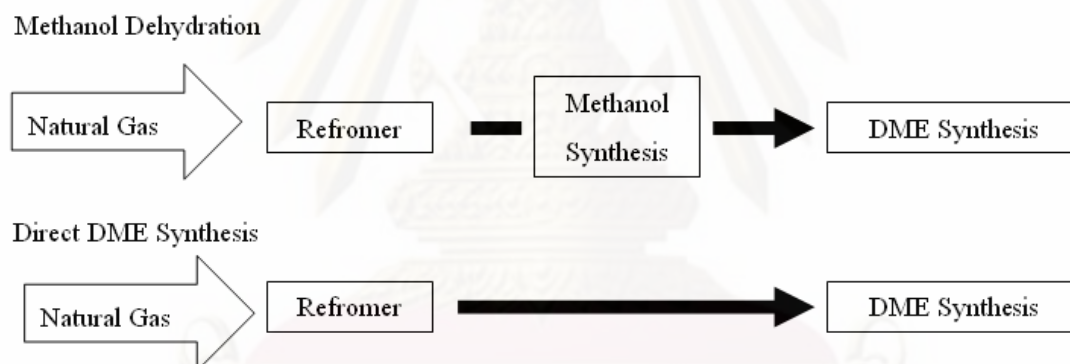


**Figure 3.2** Schematic of DME production processes [Fujimoto 2004].

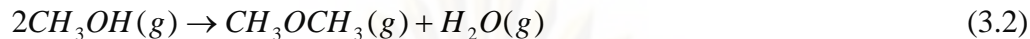
#### 3.4.1 Dimethyl ether synthesis from synthesis gas

In present, Japan produces dimethyl ether from synthesis gas. Because of synthesis gas' easy production method and their enormous resource as natural gas and coal moreover, other renewable resources like biomass used-plastic and waste water from industrial can be used also because when these resources are burned will produce synthesis gas, therefore, there will be no lacking resources problem of synthesis gas.

Dimethyl ether synthesis form synthesis gas start with methanol production from synthesis gas reaction in 3.1



Then methanol dehydration occur in 3.2 Overall dimethyl ether synthesis from synthesis gas reaction from 3.1 and 3.2 show in 3.3



However, water gas-shift reaction (WGSR) can occur from water from dehydration reaction, change carbon monoxide in synthesis gas to carbon dioxide in 3.4 and change overall dimethyl ether synthesis reaction to 3.5



Overall reactions in 3.3 and 3.5 have different ratio by mole of hydrogen and carbon monoxide, 1 and 2 respectively. When water gas-shift reaction occur equilibrium conversion is decrease. In figure 3.3 show that ratio by mole of hydrogen and carbon monoxide is 1 give the best equilibrium conversion.

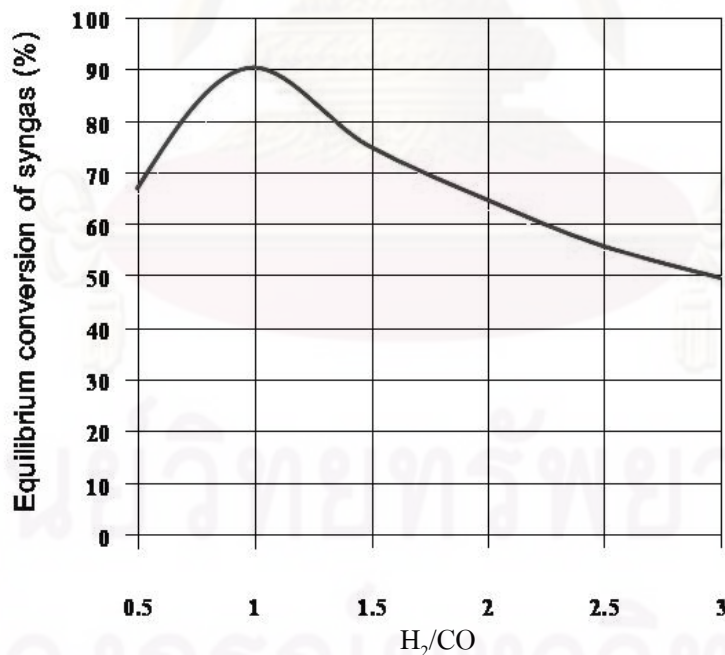
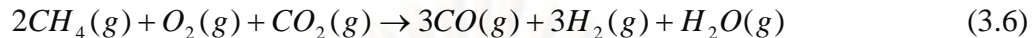


**Figure 3.3** Equilibrium conversions of synthesis gas at 260 °C and 5 MPa

[Yataro et al. 2001]

This result has good relative with ratio of synthesis gas from methane in natural gas. Carbon dioxide, by produce from methane reforming reaction can reform to carbon monoxide in 3.6

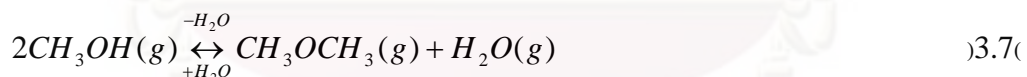


Products from this reforming reaction are carbon monoxide hydrogen and water that have ratio of carbon monoxide and hydrogen is 1, according to result in figure 3.3, Natural gas is suitable substance for dimethyl ether synthesis. [Ohno 2004 and Sudo 2002].

However, Composition of Synthesis gas, Carbon monoxide, is very expensive and has strict law to buy. dimethyl ether Synthesis consists of Methanol Dehydration reaction. So in this studies are only interest in Direct dimethyl ether synthesis from methanol.

#### 3.4.2 Direct dimethyl ether synthesis from methanol

Methanol is colorless liquid, blending homogenously with water and organic solvent, corrosive, damaged nervous system and can be dangerous if methanol enter to human body. Methanol can be used as alternative fuel substitute gasoline with less carbon monoxide, no smoke and sulfur dioxide. However, with low cetane number of methanol (about 5), methanol seldom use as fuel but usually use as substance to synthesis other higher cetane number fuel such as dimethyl ether gasoline etc. In present, dimethyl ether synthesis from methanol is widely study and in 3.7



Two molecules of methanol hydrate to dimethyl ether and water one molecule each with exothermic reaction. However, methanol can be substance in other side reactions show in figure 3.4

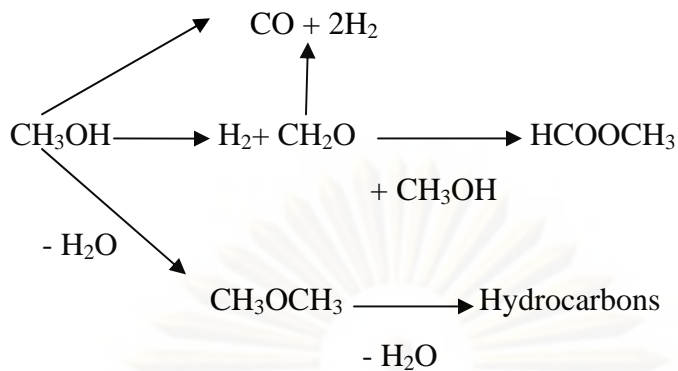
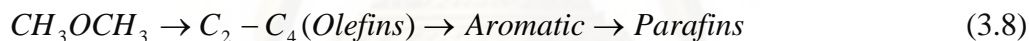


**Figure 3.4** Empirical reaction series of methanol reforming

Three main reactions from methanol are Decomposition reaction to synthesis gas, Dehydrogenation reaction that gives formaldehyde and hydrogen as product; formaldehyde can decompose to synthesis gas also or may reaction with methanol to methyl formate. Dehydration is the last main reaction that gives dimethyl ether as product however, hydrocarbon compound may occur from chain dehydration reaction of Dimethyl Ether, product form chain reaction such as light paraffin and olefin as shown in reaction 3.8 below



The most important side reaction of direct dimethyl ether synthesis from methanol is chain dehydration reaction of methanol to olefin, methanol to olefin reaction (MTO), which occur through high acidity catalyst that change ether product to hydrocarbon.

### 3.5 The Alumina

#### 3.5.1 Properties of alumina

Alumina which is  $\text{Al}_2\text{O}_3$  in general form is a polymorphic material. Alumina can be easily synthesized small particles and obtained desirous surface area and pore distribution. Commercial alumina have surface area between  $100\text{-}600 \text{ m}^2/\text{g}$ . High porosity solid cause high intra surface area, good metal dispersion and increasable effective of catalytic. There are many forms of alumina ( $\alpha$ -,  $\gamma$ -,  $\delta$ -,  $\eta$ -,  $\kappa$ -,  $\chi$ -,  $\theta$ -,  $\rho$ -, and  $\iota$ - $\text{Al}_2\text{O}_3$ ) but the  $\alpha$ - $\text{Al}_2\text{O}_3$  is the only stable form. The thermodynamically stable phase is

alpha alumina ( $\alpha$ -  $\text{Al}_2\text{O}_3$ , corundum) where all Al ions are equivalent in octahedral coordination in a hex oxide array.  $\alpha$ -  $\text{Al}_2\text{O}_3$  (corundum) powders are applied in catalysis as supports, for example, of silver catalysts for ethylene oxidation to ethylene oxide, just because they have low Lewis acidity, low catalytic activity, and conversely, they are mechanically and thermally very strong. All other alumina polymorphs are metastable. [Evans 1993].

Activated alumina has a surface with both Lewis and Bronsted acidic and basic sites. Acidity is derived from the  $\text{Al}^{3+}$  ions and  $\text{H}_2\text{O}$  molecules coordinated. Activated alumina can dry a gas to water content lower than that achievable with any other commercially available desiccant. In addition to water removal, activated alumina can be used selectively to adsorb certain other chemical species from gaseous or liquid streams. Polar molecules such as fluorides or chlorides are readily adsorbed and so activated alumina is used in petroleum refining to adsorb HCl from reformed hydrogen and organic fluorides from hydrocarbons produced by the HF-alkylation process [Evans 1993].

Activated alumina has a surface with both Lewis and Bronsted acidic and basic sites. Acidity is derived from the  $\text{Al}^{3+}$  ions and  $\text{H}_2\text{O}$  molecules coordinated to cationic sites, while basicity is due to basic hydroxide groups and  $\text{O}^{2-}$  anion vacancies [Evans 1993]. If alumina contact to humidity, surface are adsorped water molecules and when alumina were dried at  $100\text{ }^\circ\text{C}$  to  $150\text{ }^\circ\text{C}$ , water molecules are desorbed but remain hydroxyl group (-OH) cause acidity of alumina are weak Bronsted acid. (Figure 3.5) Calcination temperatures below  $300\text{ }^\circ\text{C}$ , the acid strength and concentration of alumina are low and at  $500\text{ }^\circ\text{C}$  reduce Bronsted acid sites. [Wittayakhun et al. 2004]

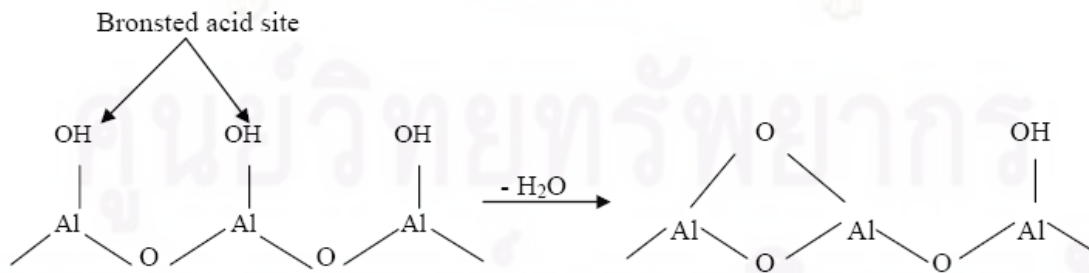


**Figure 3.5** Desorption of water from alumina surface [Wittayakhun et al. 2004].



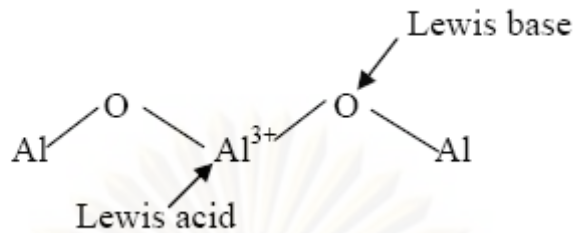


**Figure 3.6** Lewis acid and Lewis basic sites on alumina [Wittayakhun et al. 2004].

As shown in Figure 3.6, further increasing temperatures above 600 °C, adjacent –OH combine and more emit H<sub>2</sub>O and contribute to Al<sup>3+</sup> are Lewis acid sites and O<sup>2-</sup> are Lewis basic sites. Hardness of surface bring about no reaction between Lewis acid and Lewis base which both sites have high activity in various reaction such as Dehydration of alcohol and Isomerization of alkene. The decline in acidity for calcination temperatures above 800 °C can be attributed to the collapse in surface area as the alumina is converted to its alpha form [Wittayakhun et al. 2004].

### 3.5.2 Properties of $\gamma$ - Al<sub>2</sub>O<sub>3</sub> [Fierro et al.2006]

$\gamma$ - Al<sub>2</sub>O<sub>3</sub> which is the most used form of alumina in industry and any field of technologies is mostly obtained by decomposition of the boehmiteoxyhydroxide  $\gamma$ - AlOOH (giving medium surface area lamellar powders, ~100 m<sup>2</sup>/g) or of a poorly crystallized hydrous oxyhydroxide called “pseudoboehmite” at 327 to 527 °C, giving high surface area materials ( about 500 m<sup>2</sup>/g). However, the details of its structure are still matter of controversy. It has a cubic structure described by Lippens [Fierro et al. 2006] and de Boer [Fierro et al. 2006] to be a defective spinel, although, it can be tetragonally distorted. Being the stoichiometry of the “normal” spinel MgAl<sub>2</sub>O<sub>4</sub> (with Al ions virtually in octahedral coordination and Mg ions in tetrahedral coordination) the presence of all trivalent cations in  $\gamma$ - Al<sub>2</sub>O<sub>3</sub> implies the presence of vacancies in usually occupied tetrahedral or octahedral coordination sites. Soled proposed that the cation charge can be balanced, more than by vacancies, by hydroxyl ions at the surface. In fact,  $\gamma$ - Al<sub>2</sub>O<sub>3</sub> is always hydroxylated; dehydroxylation occurring only at a temperature where conversion to other alumina forms is obtained. XRD studies using the Rietveld method, performed

by Zhou [Fierro et al. 2006] and Snyder [Fierro et al. 2006], suggested that  $Al^{3+}$  cations can be in positions different from those of spinels, that is, in trigonal coordination. The possibility of a structure of  $\gamma$ - $Al_2O_3$ , as “hydrogen-spinel” has been proposed based on IR spectroscopy. Calculations based on the composition  $HAl_5O_4$  have been performed but found that this structure is very unstable. Sohlberg et al. [Fierro et al. 2006] arrived to a structure very similar to that proposed by Zhou [Fierro et al. 2006] and Snyder [Fierro et al. 2006], based on spinel but with occupation of extraspinel sites. On the contrary, Digne et al. [Fierro et al. 2006] and Krokidis et al. [Fierro et al. 2006] proposed a structure based on ccp oxide lattice but different from that of a spinel, with 25% of Al ions in tetrahedral interstice and no structural vacancies. According to these authors, this structure, although unstable with respect to corundum, is more stable than that of the spinel based structures.  $\gamma$ - $Al_2O_3$  is also active as an acidic catalyst. As for example it is very active in the dehydration of alcohols to olefins and to ether as well as both in double bond isomerization and in skeletal isomerization of olefins.

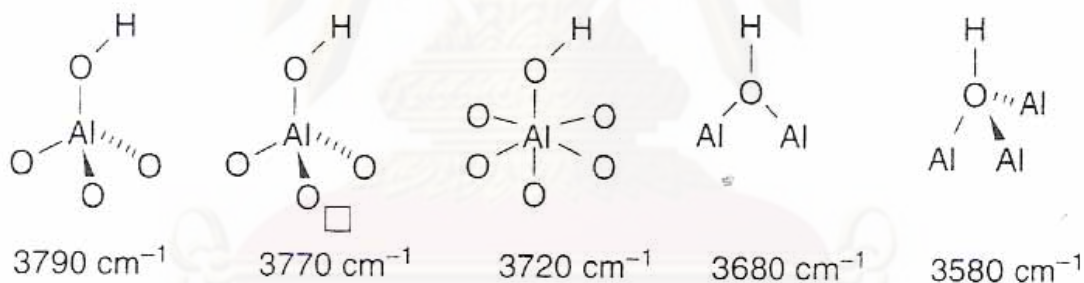


**Figure 3.7** Assignment of the OH stretchings of transitional aluminas, following Busca et al., based on the comparison with the spectra of nondefective and partially defective spinel aluminates and ferrites. The square represents a vacancy in a normally occupied position of stoichiometric spinels [Fierro et al. 2006].

In Figure 3.7 the assignments of the five main  $\nu OH$  bands of the surface hydroxyl groups of transitional aluminas proposed by Busca et al. [Fierro et al. 2006]. The catalytic activity of transitional aluminas are undoubtedly mostly related to the Lewis acidity of a small number of low coordination surface aluminum ions, as well as to high ionicity of

the surface Al-O bond. The alumina's Lewis sites have been well characterized by adsorption of probes such as pyridine, carbon monoxide, and several bases followed by IR, ammonia and amines followed by calorimetric, triphenylphosphine followed by  $^{31}\text{P}$  NMR, to be the strongest among metal oxides, only weaker than those of Al halides. Volumetric, TPD and calorimetric experiment allowed also to determine the amount of such very strong Lewis sites present on transitional alumina surfaces, which however depend on the dehydroxylation degree (depending on the activation temperature) and the peculiar phase and preparation [Fierro et al. 2006].

### 3.6 Aluminum Phosphate

Aluminum phosphate ( $\text{AlPO}_4$ ) or Aluminum Orthophosphate is white crystal solid in ambient and room temperature, melting point of  $\text{AlPO}_4$  is above  $1500^\circ\text{C}$ ; insoluble in water, soluble in acids and bases. In industrial, aluminum phosphate is very useful in ceramics paint pulp and paper. However, aluminum phosphate has been used in catalysis as well and could be separated by their structures, amorphous and crystalline, which have different properties and term of used.

Recently, amorphous aluminum phosphate structure is found that has a property to be dehydration catalyst from modification of alumina with phosphate group. Amorphous aluminum phosphate was found that had higher surface area and significant acidity especially more than crystalline one. Moreover, activity of amorphous aluminum phosphate in methanol dehydration was very close to  $\gamma\text{-Al}_2\text{O}_3$  which some study report that it gave less by-product. However, crystalline aluminum phosphate was used in catalysis either.

Aluminum phosphate in crystalline structure might be known as Aluminophosphates ( $\text{AlPO}_4$ s) are crystalline microporous molecular sieves. They are made up from alternating  $\text{AlO}_4$  and  $\text{PO}_4$  tetrahedral, connected through corner sharing of oxygen atoms. These tetrahedral moieties then form a three-dimensional network containing channels and pores.  $\text{AlPO}_4$ s are structurally analogous to the type of aluminosilicate zeolites which is one type of zeotype, molecules which have a similar structure as zeolite but consist of different element such as  $\text{AlPO}_4$ s and  $\text{SaPO}_4$ s, where the

$\text{Si}^{4+}$  can be substituted by  $\text{P}^{4+}$  to have an alternate arrangement of Al and P. AIPOs, though a structural analog of zeolite the show a better flexibility than zeolites towards chemical substitution. Moreover, beside of molecular sieves AIPOs could be used as a blending agent of commercial zeolites catalyst in industrial also. [Chatterjee 2006]



ศูนย์วิทยทรัพยากร  
จุฬาลงกรณ์มหาวิทยาลัย

## CHAPTER IV

### EXPERIMENTAL

This chapter consists of experimental systems and procedures used in this work which is divided into three parts. The catalyst preparation of aluminum phosphate and gamma alumina with contains chemical, equipment and procedure in section 4.1. Section 4.2 describes the details of catalyst characterization by various techniques such as X-ray diffraction (XRD), N<sub>2</sub> physisorption, ammonia temperature programmed desorption (NH<sub>3</sub>-TPD), thermogravimetric and differential thermal analysis (TG-DTA), Fourier transform infrared (FT-IR), Fourier transform Raman (FT-Raman) and amine titration using Hammett indicators. The last part (section 4.3) describes the catalytic test in methanol dehydration to dimethyl ether (DME).

#### 4.1 Catalyst preparation

The synthesis catalysts in this study were amorphous aluminum phosphate and solvothermal gamma alumina. The commercial gamma alumina is alumina oxide for chromatography (fluka).

##### 4.1.1 Preparation of amorphous aluminum phosphate catalyst by precipitation method

In this study, the modified Bautista's aqueous solution precipitation method [Bautista, 2005] was chosen as catalyst preparation method. The details of chemicals and method for preparation of amorphous aluminum phosphate have shown as follows:

Aluminum nitrate, (Al(NO <sub>3</sub> ) <sub>3</sub> ·9H <sub>2</sub> O)	analytical grade, Aldrich
Phosphoric acid, (85% H <sub>3</sub> PO <sub>4</sub> )	analytical grade, Aldrich
Aqueous ammonia solution, (25% NH <sub>4</sub> OH)	analytical grade, Merck
2-Propanol, (C <sub>3</sub> H <sub>5</sub> OH)	analytical grade, Fisher Scientific

Preparation of 6 grams of amorphous aluminum phosphate, 18.45 grams of aluminum nitrate was diluted in 30 ml of deionization water to prepared aluminum precursor solution. Mixing and stirring this aqueous solution at controlled temperature of 0°C, equal molar amount of phosphate precursor, 1.68 ml of phosphoric acid was added to form amorphous aluminum phosphate with have Al/P ratio =1. Aqueous ammonia solution was added dropwise to precipitation of aluminum phosphate until pH of solution = 7. The solution would changed from homogenous to gelled mass meanwhile pH adjustment and rapidly viscous when pH closed to 7. Notice that neutralization of acid-base has generated amount of heat, make sure that controlled temperature was constant. Filtration and wash catalyst gel with vacuum filter and deionization water to remove excess substance and contaminant. Wash again with 2-propanol and dried at 100°C for 24 hour. The resulting catalyst would be calcined at 650°C in air for 3 hours to air atmosphere.

#### 4.1.2 Preparation of gamma alumina catalyst by solvothermal method

Synthesis gamma alumina method was using preparation method of various phases of alumina supports (gamma phase, chi phase and their mixed-phase) by solvothermal [Khom-in, 2007]. The details of chemicals, equipment (autoclave reactor line) and method for preparation of pure gamma alumina by solvothermal method have shown as follows:

Alumina Isopropoxide: AIP, $[(\text{CH}_3)_2\text{CHO}]_3\text{Al}$	analytical grade, Aldrich
1-Butanol, $(\text{C}_4\text{H}_9\text{OH})$	analytical grade, Fluka
Methanol, $(\text{CH}_3\text{OH})$	commercial grade, Merck
Nitrogen gas, $(\text{N}_2)$	ultra high purity, TIG

In this study, stainless steel autoclave reactor was connected to pressure gauge with relief valve to prevent runaway reaction. Test tube was used to contain the reagent and solvent inside autoclave reactor. In condition of 15 g of amount of starting material and 100 ml of organic solvent was contained in the test tube with another 30 ml of organic solvent in the gap between test tube and autoclave wall. Thermocouple is attached to the

reagent in the autoclave. Autoclave reactor used for the experiment is shown in Figure 4.1.

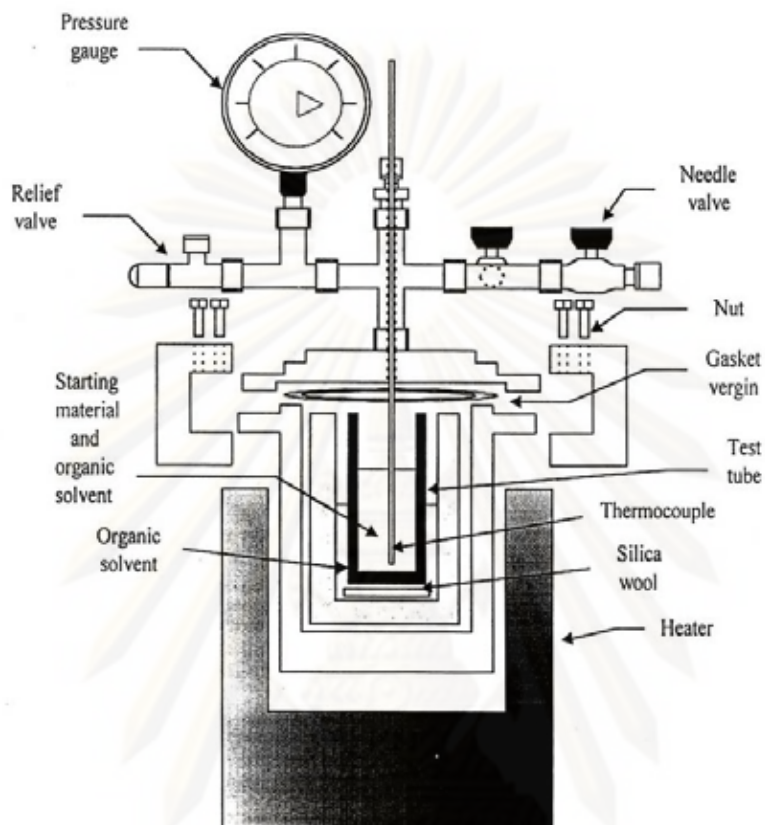


**Figure 4.1** Autoclave reactor

Moreover, temperature program controller was connected to a thermocouple attached to the autoclave with electrical furnace supplied the required heat to the autoclave for the reaction. Nitrogen was set with a pressure regulator (0-150 bar) and needle valves were used to release gas from autoclave. The diagram of the reaction equipment for the synthesis of catalyst is shown in Figure 4.2

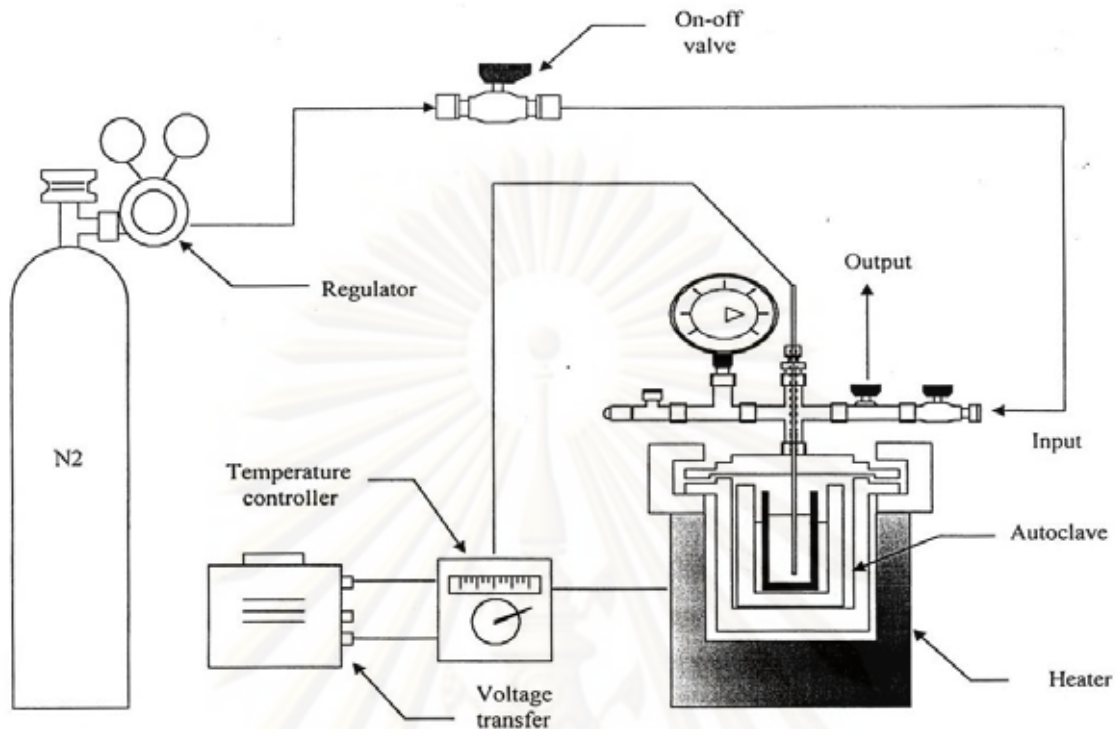


**Figure 4.2** Diagram of the reaction equipment for the synthesis of catalyst.

The equipment for the synthesis of alumina by solvothermal method consisted of: 15 g of aluminum isopropoxide was suspended in 100 ml of desired organic solvent in a test tube, the organic solvents using in this experiments were toluene, 1-butanol and the mix solvents between both solvents with desired composition, and then the test tube was placed in a 300 ml autoclave. An addition 30 ml of same solvent was placed in the gap between the autoclave wall and the test tube. The autoclave was completely purged with nitrogen, heated to a desired temperature at a rate of  $2.5\text{ }^{\circ}\text{C min}^{-1}$  and kept at that temperature for 2 h. After the autoclave was cooled to room temperature, the resulting product was repeatedly washed with methanol by vigorous mixing and centrifuging and then dried in air. The as-synthesized powders were calcined in air at  $600\text{ }^{\circ}\text{C}$  for 6 h with a heating rate of  $10\text{ }^{\circ}\text{C/min}$ . [J.Khom-in, 2007]



## **4.2. Catalyst characterization**

### **4.2.1 X-ray diffraction pattern**

The crystallinity of the prepared catalysts was identified using powder X-ray diffraction (XRD) by an X-ray diffractometer SIEMENS D 5000 connected with a personal computer with Diffract AT version 3.3 program for fully control of the XRD analyzer. The experiments were carried out by using Ni-filtered Cu  $K_{\alpha}$  radiations with a generator voltage and current of 30 kV and 30 mA, respectively. A scan step of  $0.04^{\circ}$  was applied during a continuous run in the  $20-70^{\circ}$  range.

### **4.2.2 Nitrogen physisorption**

The catalyst 0.2 gram was study BET surface area, pore volume and pore diameter were measured by  $N_2$  adsorption–desorption isotherm at liquid nitrogen temperature ( $-196^{\circ}\text{C}$ ) using a Micromeritics ASAP 2020. The surface area and pore distribution were calculated according to Brunauer-Emmett-Teller (BET) and Barret-Joyner-Halenda (BJH) methods, consecutively.

### **4.2.3 Temperature Programmed Desorption of Ammonia ( $\text{NH}_3$ -TPD)**

The acid properties of prepared catalysts were observed by Temperature Programmed Adsorption of Ammonia ( $\text{NH}_3$ -TPD) equipment by using Micromeritics chemisorp 2750 Pulse Chemisorption System. In an experiment, about 0.10 g of the catalyst sample was placed in a quartz tube and pretreated at  $200^{\circ}\text{C}$  in a flow of helium. The sample was saturated with 15%  $\text{NH}_3/\text{He}$ . After saturation, the physisorbed ammonia was desorped in a helium gas flow about 1.0 h. Then the sample was heated from 40 to  $800^{\circ}\text{C}$  at a heating rate  $10^{\circ}\text{C}/\text{min}$ . The amount of ammonia in effluent was measured via TCD signal as a function of temperature.

#### 4.2.4 Thermogravimetric and differential thermal analysis (TG-DTA)

The as-spun alumina fibers was subjected to the thermogravimetric and differential thermal analysis (Diamond Thermogravimetric and Differential Analyzer, TA Instruments SDT Q600) to determine the carbon content in the sample, as well as their thermal behaviors in the range of 10-800 °C. The analysis was performed at a heating rate of 10 °C /min in 100 ml/min flow of air.

#### 4.2.5 Fourier transform infrared (FT-IR)

Fourier transform infrared (FT-IR) were performed to identify the hydroxyl groups of catalysts. Infrared survey was recorded by using Nicolet 6700<sup>TM</sup> spectrometer in the range of 4000-400 cm<sup>-1</sup> at a resolution of 2.0 cm<sup>-1</sup>.

#### 4.2.6 Fourier transform Raman (FT-Raman)

Fourier transform Raman (FT-Raman) were performed to identify the phosphate groups of catalysts using Perkin Elmer, spectrum GX in the Raman shift range of 200-3600 cm<sup>-1</sup> at a resolution of 4.0 cm<sup>-1</sup>

#### 4.2.7 Amine titration using Hammett indicators [Yurdakoc, 1999]

The acid strength of a solid surface is defined as the ability of the surface to convert an adsorbed neutral base into its conjugate acid. If the reaction proceeds by means of proton transfer from the surface to the adsorbate, the acid strength is quantitatively expressed by Hammett and Deyrup's H<sup>0</sup> acidity equation 4.1.

$$H^0 = pK_a + \log[B]/[BH^+] \quad (4.1)$$

Where [B] and [BH<sup>+</sup>] are the concentrations of the neutral base and its conjugate acid respectively, and pK<sub>a</sub> is pK<sub>BH<sup>+</sup></sub>. If the reaction takes place by means of the electron pair transfer from the adsorbate to the surface, H<sup>0</sup> is expressed by equation 4.2.

$$H^0 = pK_a + \log[B]/[AB] \quad (4.2)$$

Where [AB] is the concentration of the neutral base which reacted with the Lewis acid or electronpair acceptor, A. The amount of acid on a solid is usually expressed as the number or mmol of acid sites per unit weight or per unit surface area of the solid. In the amine titration method using indicators, the color of suitable indicators adsorbed on the surface will give a measure of its acid strength. If the color is that of the acid form of the indicator, then the value of the  $H^0$  function of the solid is equal to or lowers than the  $pK_a$  of the conjugate acid of the indicator.

The Hammett indicators used in the present study are listed in Table 4.1, together with color changes and  $pK_a$ 's. Moreover, to give some idea of the acid strength range, corresponding sulfuric acid compositions are also listed.

Acid Amount Determination, samples should be freshly dried at 393K before carrying out the indicator tests, and were subjected to color immediately after drying, or if this was not convenient, were stored in screw cap test tubes in a desiccators until color tests were performed. Since water is a base, the effect of water adsorption changed the color intensities of the adsorbed indicators or caused a shift to lower acid strengths.

Amine titration using Hammett indicators carried out. 0.1 g of catalyst was suspended in 9 ml of benzene with 3 dropwise of Hammett indicators; indicator solution was prepared by diluted 0.1 g of indicator in 100 ml of non-polar organic solvent. If suspension catalyst solution has color of acid form of indicators, the catalyst had more acid strength than  $pK_a$  of indicators, titrated to measured the acid amount with 0.01 M of n-butylamine in benzene solution until color of solution changed to base form, than the solution was shaken for at least 2 hour, if color changed to acid form, titrated again with same procedure until color turned to base form permanently. Strength and amount of acid sites reported in range depending on amount and type of used Hammett indicators.

**Table 4.1** Basic indicators used for the measurement of acid strength

Indicator	Color Base Form	Color Acid Form	pK <sub>a</sub>
Neutral Red	yellow	red	+6.8
Methyl Red	yellow	red	+4.8
Methyl Orange	yellow	orange	+3.7
Phenylazonaphthylamine	yellow	red	+4.0
p-Dimethylaminoazobenzene (Methyl Yellow)	yellow	red	+3.3
2-Amino-5-azotoluene	yellow	red	+2.0
Benzeneazodiphenylamine	yellow	purple	+1.5
Crystal Violet	blue	yellow	+0.8
p-Nitrobenzeneazo-(p'-nitro-diphenylamine)	orange	purple	+0.43
Dicinnamalacetone	yellow	red	-3.0
Benzaacetophenone	colorless	yellow	-5.6
Anthraquinone	colorless	yellow	-8.2
2,4,6-Trinitroaniline	colorless	yellow	-10.1

\* The indicator is liquid at room temperature and acid strength corresponding to the indicator is higher than the acid strength of 100 percent H<sub>2</sub>SO<sub>4</sub>.

### 4.3 Reaction study in dehydration of methanol

#### 4.3.1 Chemical and Reagents

UHP Helium Gas, 99.999% as carrier gas of reaction test

Methanol, (CH<sub>3</sub>OH) from Merck as reactant

Distillation water, (H<sub>2</sub>O)

### 4.3.2 Instrument and Apparatus

The equipment for the reaction of aluminum phosphate and gamma alumina consisted of: The flow diagram of the reaction that is methanol dehydration to dimethyl ether is shown in Figure 4.6

(a) Reactor: Reactor tube was made from pyrex and had an inner diameter 6 mm and height 39.5 cm.

(b) Saturator: Saturator was made from glass and set to bubble methanol and control pressure of methanol. Moreover, saturator was set to feed water vapor to pretreatment catalysts before reaction test.

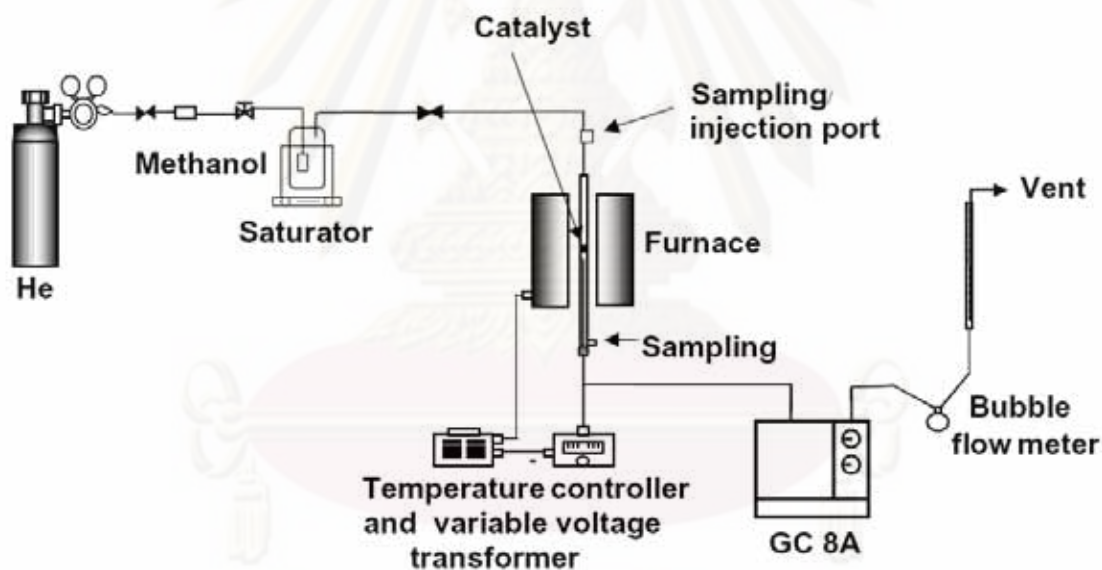


**Figure 4.3** A schematic of methanol dehydration system

(c) Heater and furnace: Heating cable was used to heat temperature of line preventing condensation of methanol. Variable voltage transformer was used to control the desired reactor temperature of furnace.

(d) Temperature program controller: A temperature program controller was connected to a thermocouple attached to the reactor and variable voltage transformer and controlled the temperature.

(e) Gas controlling system: Helium was set with a pressure regulator (0-150 bar) and regulator was used to release gas to line.

(f) Gas chromatography (GC): Shimadzu model 8AIT was established for analyzing the reaction products with thermal conductivity detector (TCD). The TCD measures the conductivity of the analyte mixture which is a function of the concentration of the analyte in the gas. A carrier gas was Helium (He) and column were Porapak Q and Porapak N (3 m×3 mmØ) for analyzing the concentration of methanol (CH<sub>3</sub>OH), water (H<sub>2</sub>O) and dimethyl ether (CH<sub>3</sub>OCH<sub>3</sub>) with different by-production, Porapak Q for CH<sub>4</sub> CO<sub>2</sub> and light olefins, Porapak N for CO and CH<sub>4</sub>. Operating conditions were shown in Table 4.3.

As shown in Figure 4.3, the diagram of methanol dehydration was used to investigate catalytic test. Catalytic experiments were performed at atmosphere pressure in fixed-bed reactor consisting of a Pyrex tube, a coaxially centered thermocouple with its tip located in the middle of the bed. The dehydration of methanol over the catalyst samples was carried out in reactor with an inner diameter 6 mm. In an experiment, 0.2 g of each catalyst was loaded and the gas hourly space velocity (GHSV) was 5,300 h<sup>-1</sup>. Methanol was bubbled by helium through a glass saturator maintained at 29 °C to keep a feed gas mixture consisting of 20% methanol balanced in helium. The partial pressure of methanol in the gas mixture was 169 mmHg. The calculation of the partial pressure of methanol was shown in Appendix A. The reactor was carried out in the temperature range: 150-300°C under atmospheric pressure. The reaction products were analyzed with a gas chromatograph with a TCD detector and a Porapak-Q and Porapak-N column were operating at 110°C and 100°C [Ng 2002].

**Table 4.3** Operating condition gas chromatograph for methanol dehydration reaction

Gas Chromatograph	Shimazu, GC 8A	Shimazu, GC 8A
Detector	TCD	TCD
Column	Porapak-Q	Porapak-N
Carrier gas	Helium (UHP)	Helium (UHP)
Carrier gas flow	50 ml/min	30 ml/min
Column Temperature		
- Initial	110°C	100°C
- Final	110°C	100°C
Detector temperature	110°C	100°C
Injector Temperature	110°C	100°C
Analyzed gas	CH <sub>3</sub> OH, H <sub>2</sub> O, DME, CO <sub>2</sub> and light olefins	CH <sub>3</sub> OH, H <sub>2</sub> O, DME, CO and CH <sub>4</sub>

The product gas composition was analyzed by a Shimadzu gas chromatograph (GC). The GC was equipped with a thermal conductivity detector (TCD). Helium was used as the carrier gas and separation of the constituents was achieved using molecular both Porapak column. Porapak Q and Porapak N were used to analyze feed reactant and major product; CH<sub>3</sub>OH, H<sub>2</sub>O and DME with different by-production, Porapak Q for CH<sub>4</sub> CO<sub>2</sub> and light olefins, Porapak N for CO and CH<sub>4</sub>. The calibration curves for calculation of composition of reactant and products in methanol dehydration were shown in Appendix B.

## CHAPTER V

### RESULTS AND DISCUSSIONS

The catalyst including amorphous  $\text{AlPO}_4$ , solvothermal  $\gamma\text{-Al}_2\text{O}_3$ , and commercial  $\gamma\text{-Al}_2\text{O}_3$  were performed in methanol dehydration reaction. The  $\text{AlPO}_4$  was tested for the effect of water pretreatment under various conditions. This chapter is divided into three sections. The first section contains characterization of the fresh catalysts. The second section shows methanol dehydration tests of catalyst. The last section presents the characterization of treated  $\text{AlPO}_4$  in order to investigate the water pretreatment effect on the catalyst behavior.

For catalyst characterization, fresh catalysts were characterized by XRD, BET, and  $\text{NH}_3$ -TPD. Treated catalysts were characterized by TGA, FT-IR, FT-Raman, and amine titration using Hammett indicators. For methanol dehydration test, the reaction was carried out at the temperature range  $150^\circ\text{C}$  to  $300^\circ\text{C}$  and atmospheric pressure.

#### 5.1 Characterization of fresh catalysts

##### 5.1.1 X-ray Diffraction (XRD)

Bulk crystal structure and chemical phase composition of a crystalline material can be detected by diffraction of an X-ray beam as a function of the angle of the incident beam. In addition, if material has structure of amorphous, the X-ray beam would scattered and gave a little diffraction quantity of X-ray beam from material which showed very low intensity of XRD Diffraction pattern. The measurements were carried out at the diffraction angles ( $2\theta$ ) between  $20$  and  $70$  degrees.

The XRD Diffraction patterns for amorphous  $\text{AlPO}_4$ , solvothermal  $\gamma\text{-Al}_2\text{O}_3$ , and commercial  $\gamma\text{-Al}_2\text{O}_3$  has shown in Figure 5.1. The patterns indicated that the nature structure of  $\text{AlPO}_4$  was amorphous and both commercial and synthetic  $\gamma\text{-Al}_2\text{O}_3$  were



crystal structure of which indicated obviously at degree  $2\theta$  of  $32^\circ$ ,  $37^\circ$ ,  $39^\circ$ ,  $45^\circ$ ,  $61^\circ$  and  $66^\circ$  indicating the pure  $\gamma$ - phase of alumina [Khom-In, 2008].

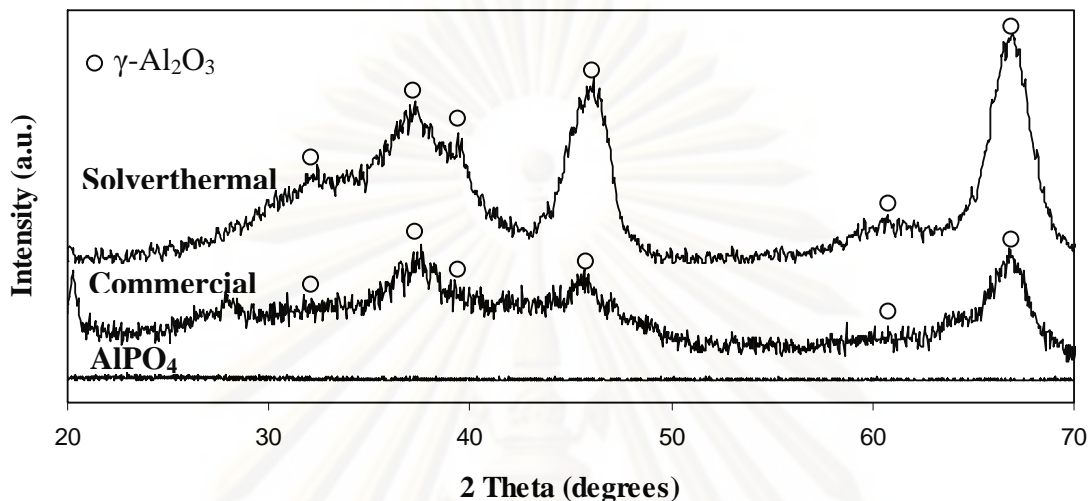


**Figure 5.1** XRD patterns of amorphous  $\text{AlPO}_4$ , solvothermal  $\gamma\text{-Al}_2\text{O}_3$ , and commercial  $\gamma\text{-Al}_2\text{O}_3$

### 5.1.2 Nitrogen physisorption

The most common procedure for determining specific surface area, pore size and pore volume of solid material are based on adsorption and condensation of nitrogen at liquid phase temperature. The specific surface area was calculated by BET (Brunauer Emmett Teller) equation method.

The physical properties of amorphous  $\text{AlPO}_4$ , solvothermal  $\gamma\text{-Al}_2\text{O}_3$ , and commercial  $\gamma\text{-Al}_2\text{O}_3$  such as BET surface areas, pore volume and pore radius were collected in Table 5.1. The solvothermal  $\gamma\text{-Al}_2\text{O}_3$  showed higher surface area than the commercial one while  $\text{AlPO}_4$  showed the highest surface area and the largest pore size and pore volume.

**Table 5.1** Physical properties of amorphous  $\text{AlPO}_4$ , synthesis and commercial  $\text{Al}_2\text{O}_3$ 

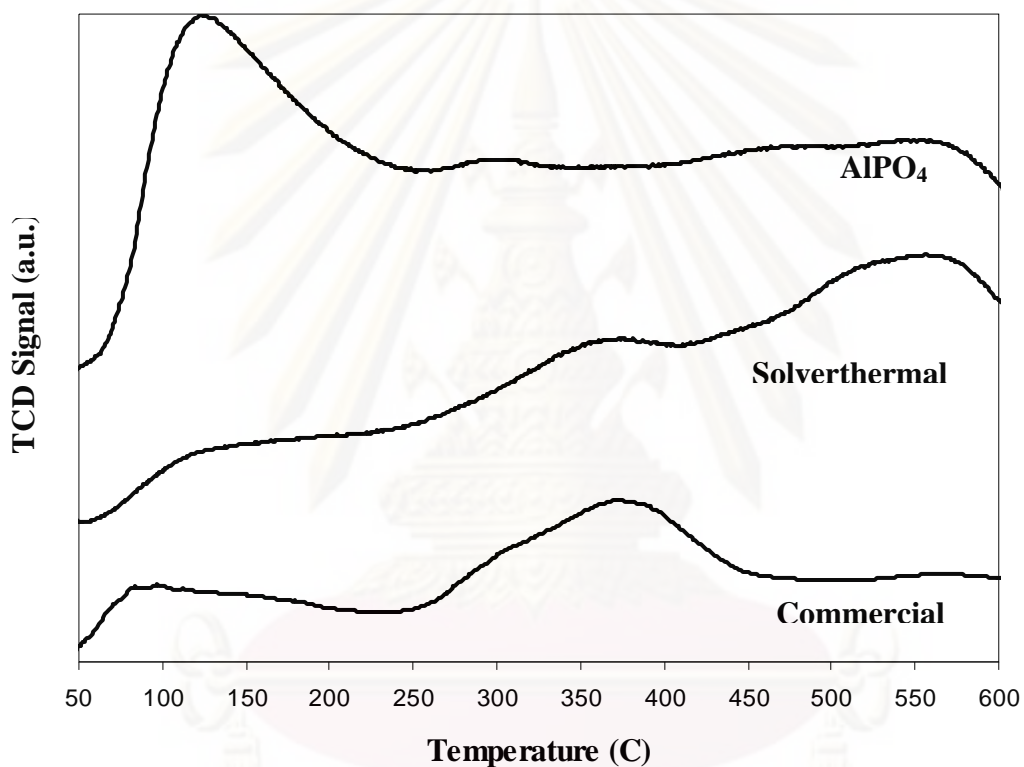
Catalyst	Specific surface area ( $\text{m}^2/\text{g}$ )	Pore volume ( $\text{cm}^3/\text{g}$ )	Pore radius ( $\text{\AA}$ )
Amorphous $\text{AlPO}_4$	171	0.76	177.1
Solvothermal $\gamma\text{-Al}_2\text{O}_3$	159	0.44	81.4
Commercial $\gamma\text{-Al}_2\text{O}_3$	149	0.23	37.0

### 5.1.3 Ammonia Temperature Programmed Desorption ( $\text{NH}_3$ -TPD)

Acidity of catalyst was indicated by adsorption of saturated  $\text{NH}_3$  on the the catalyst surface. Amount of  $\text{NH}_3$  desorption determined from peak area shows number of acid sites and desorption temperature shows bonding strength or strength of acidity of the catalyst. The  $\text{NH}_3$ -TPD profiles for amorphous  $\text{AlPO}_4$ , solvothermal  $\gamma\text{-Al}_2\text{O}_3$ , and commercial  $\gamma\text{-Al}_2\text{O}_3$  have shown in Figure 5.2. The result shows that  $\text{AlPO}_4$  had large broad peak at temperature of  $50^\circ\text{C}$  to  $250^\circ\text{C}$ , representing weak acid sites which were much higher than strong acid sites at high temperature. Solvothermal  $\gamma\text{-Al}_2\text{O}_3$  showed 3 broad peaks during the temperature range of  $50$  to  $240^\circ\text{C}$ ,  $240$  to  $450^\circ\text{C}$ , and  $480$  to  $600^\circ\text{C}$ , respectively. The profile was referred to strong acid sites with larger peaks at higher temperature above  $400^\circ\text{C}$ . The commercial  $\gamma\text{-Al}_2\text{O}_3$  shows only 2 broad peaks during the temperature range of  $50$  to  $240^\circ\text{C}$  and  $240$  to  $450^\circ\text{C}$ , indicating the acid strength between  $\text{AlPO}_4$  and solvothermal  $\gamma\text{-Al}_2\text{O}_3$ . The acid properties of catalysts are also reported in Table 5.2. The calculation of the acidity is shown in Appendix C. The total amount of acidity of the catalysts were increased in the order of amorphous  $\text{AlPO}_4$  ( $35.82 \text{ mmol H}^+/\text{g catalyst}$ ) > solvothermal  $\gamma\text{-Al}_2\text{O}_3$  ( $21.56 \text{ mmol H}^+/\text{g catalyst}$ ) > commercial  $\gamma\text{-Al}_2\text{O}_3$  ( $10.14 \text{ mmol H}^+/\text{g catalyst}$ ), respectively.

**Table 5.2** Acidity of amorphous  $\text{AlPO}_4$ , synthesis and commercial  $\text{Al}_2\text{O}_3$ 

Catalyst	Adsorbed volume of ammonia, (ml)	Total acid site, (mmol $\text{H}^+$ /g)
Amorphous $\text{AlPO}_4$	87.6	35.82
Solvothermal $\gamma\text{-Al}_2\text{O}_3$	52.71	21.56
Commercial $\gamma\text{-Al}_2\text{O}_3$	24.8	10.14

**Figure 5.2**  $\text{NH}_3$ -TPD Profiles of amorphous  $\text{AlPO}_4$ , commercial  $\gamma\text{-Al}_2\text{O}_3$  and synthetic solvothermal  $\gamma\text{-Al}_2\text{O}_3$  catalysts.

## 5.2 Reaction Study

### 5.2.1 Step-up and step-down temperature reaction test

Result of reaction test have shown that amorphous  $\text{AlPO}_4$  and solvothermal synthesize  $\gamma\text{-Al}_2\text{O}_3$  have significantly higher activity than the commercial catalyst as

illustrated in Figure 5.3. Activity of catalysts directly increased with rising temperature as the kinetic energy of the system increased with increasing temperature. Both of the synthesized catalysts ( $\text{AlPO}_4$  and solvothermal  $\gamma\text{-Al}_2\text{O}_3$ ), the reaction started to occur at  $200^\circ\text{C}$  and had a sharp increasing of methanol conversion at  $250^\circ\text{C}$ . However, activity of amorphous  $\text{AlPO}_4$  was slightly decreased at  $300^\circ\text{C}$  due to decreasing of equilibrium conversion of methanol dehydration reaction, exothermic reaction, at high temperature after reaction has reached equilibrium conversion at  $250^\circ\text{C}$ . The trend of activity of  $\text{AlPO}_4$  synthesis and commercial  $\gamma\text{-Al}_2\text{O}_3$  were followed their amount of acidity and surface area as determined from  $\text{NH}_3\text{-TPD}$  and  $\text{N}_2$  adsorption respectively. Moreover, all the three catalysts gave almost 100% selectivity of DME with less than 1% of by product such as carbon monoxide and methane.

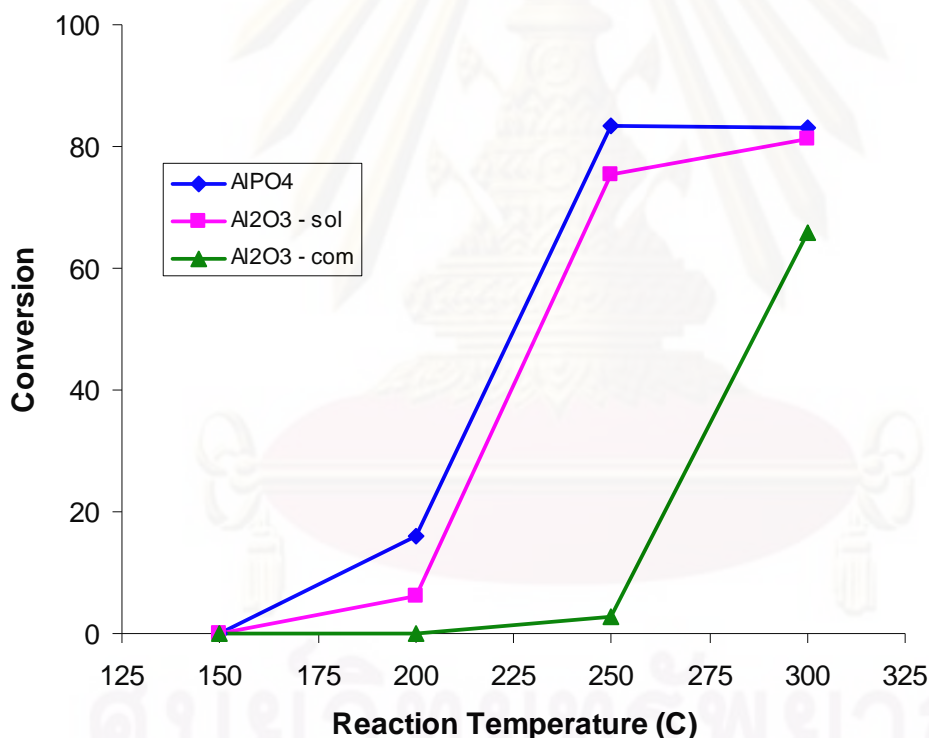


**Figure 5.3** Methanol conversion profile of step-up reaction temperature (0.2 g catalyst,  $\text{GHSV}=5,300 \text{ h}^{-1}$ )

However, further experiment has shown an interesting result when reaction temperature direction changed from  $150^\circ\text{C}$  to  $300^\circ\text{C}$  (step-up temperature) to be  $300^\circ\text{C}$  to  $150^\circ\text{C}$  (step-down temperature). The temperature was first raised to  $300^\circ\text{C}$  and step-

down to 150°C. Figure 5.4 showed the activity profile of catalysts during step-down reaction temperature test.

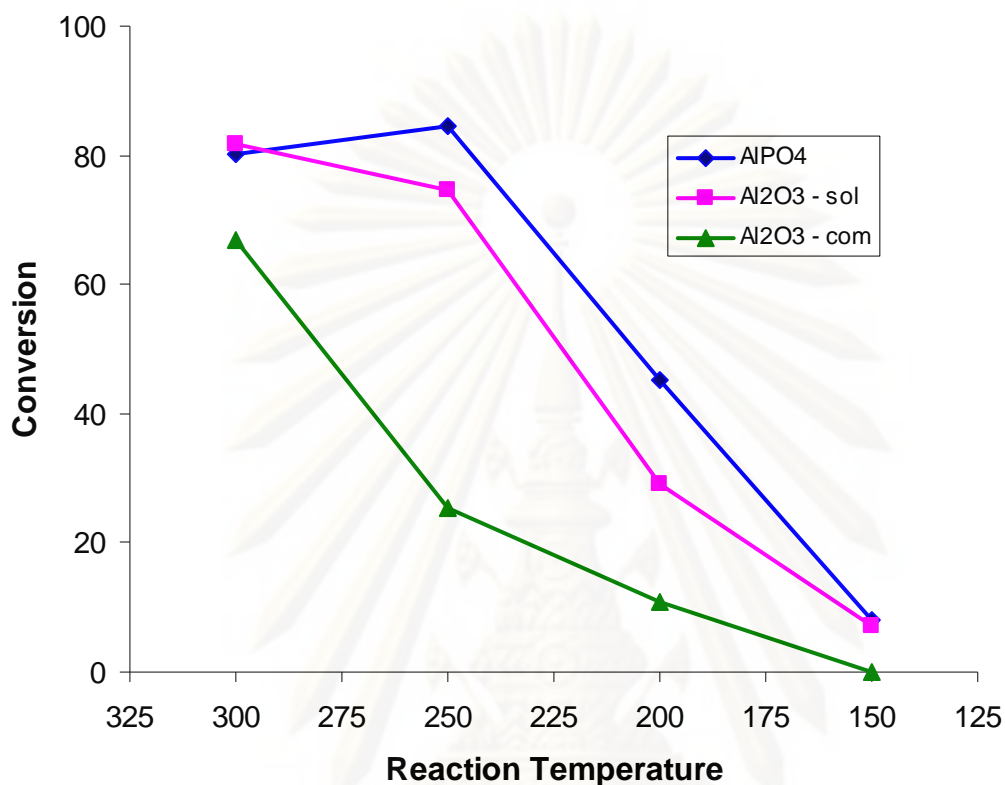


**Figure 5.4** Methanol conversion profile of step-down reaction temperature (0.2 g catalyst, GHSV=5,300 h<sup>-1</sup>)

As shown in Figure 5.4, the step-down temperature reaction test gave different results in the same trend of activity of all catalysts, increasing of activity compared to the step-up temperature reaction. Both of synthesized catalysts still showed the same methanol conversion results at 300°C and 250°C as those of step-up temperature reaction test, however, at the temperature of 200°C, the methanol conversion were significantly increased from 15.3% to 45.1% for the amorphous AlPO<sub>4</sub> and 6.0% to 29.1% for the solvothermal synthesized  $\gamma$ -Al<sub>2</sub>O<sub>3</sub>. Moreover, there were some activities at 150°C during step-down temperature test while there was no reaction occurred in this temperature in step-up temperature reaction test. The commercial  $\gamma$ -Al<sub>2</sub>O<sub>3</sub> also showed an increasing of methanol conversion from 3% to 25% at temperature of 250°C and up to 11% at 200°C.

The step-down reaction test gave the same DME selectivity as those of the step-up temperature test.

### 5.2.2 Water pretreatment of $\text{AlPO}_4$ catalyst

Because of the reason that there was no different manner in reaction test except the temperature direction from step-up temperature to step-down temperature, the hypothesis of activity increasing was suggest being either the high temperature pretreatment or the presence of water product during dehydration reaction. Further experiment was carried out in order to prove our hypothesis. The amorphous  $\text{AlPO}_4$  was activated at  $300^\circ\text{C}$  in neutral atmosphere of helium for 1 hour before the testing catalyst activity at  $200^\circ\text{C}$ . The result showed that there was no increasing of activity after heating pretreatment alone so the high temperature pretreatment hypothesis was declined.

Although, there have been many studies reported that water was the poison in this reaction and caused the decreasing of activity [Jun, 2002 and Xu, 1997], some studies reported opposite result that water could help increasing of catalyst activity in dehydration reaction. One of reasonable hypotheses are that if there was water in reaction, Lewis acid sites could be changed to Brønsted acid sites which is stronger acidity than Lewis one so that catalytic activity could be improved also [Ludmány, 2004]. Moreover, phosphate catalyst gave a promising property to resist presence of water that occurs during methanol dehydration reaction according to a study reported by András et al. [Ludmány, 2004]. As a reason, we believe that water product occurred during reaction is the major factor of activity increasing of the catalysts.

The effect of water pretreatment on  $\text{AlPO}_4$  catalyst was then investigated under various pretreatment conditions. Methanol reactant in glass saturator was substituted by distillation water and was bubbled by helium through catalyst in reactor as water vapor phase at the same GHSV of  $5,300 \text{ h}^{-1}$  before reaction test. The temperature was varied at 100, 200, 250 and  $300^\circ\text{C}$ . The amount of water pretreatment was controlled by vapor pressure of water and was varied from 5% to 20% by maintaining at  $33^\circ\text{C}$  to  $61^\circ\text{C}$  according to Antoine's equation. The pretreatment time was fixed at 15 minutes. The

results of effect of water pretreatment temperature of treated and non-treated  $\text{AlPO}_4$  are shown in Figure 5.5.

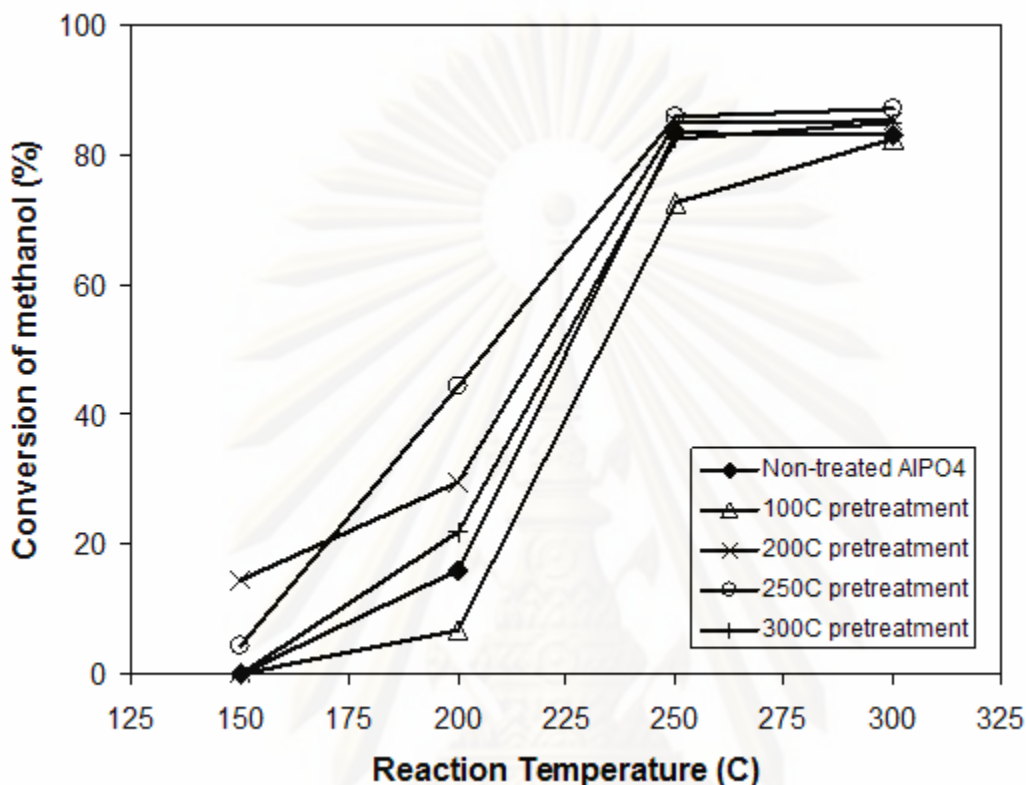


**Figure 5.5** Effect of water pretreatment temperature of treated and non-treated amorphous  $\text{AlPO}_4$  (0.2 g catalyst, GHSV=5,300  $\text{h}^{-1}$ , 10% mol water 15 minute pretreatment)

The result of water pretreatment of  $\text{AlPO}_4$  before reaction test gave a higher activity compared with non-treated  $\text{AlPO}_4$ , except the result of 100°C pretreatment that gave lower activity. The water pretreatment also gave almost 100% DME selectivity. The effect of water pretreatment temperature showed both result that water could be poison or an effective way to increased activity of catalyst in dehydration of methanol reaction, depending on the conditions of pretreatment. At 100°C pretreatment, the presence of water molecule in reaction probably could not fully bond with active sites of  $\text{AlPO}_4$ , resulting in blocking of methanol from adsorption on the active sites and became a cause of catalyst deactivation. Higher pretreatment temperature gave better activity than

fresh  $\text{AlPO}_4$ . The methanol conversion increasing in the order of pretreatment temperature  $250^\circ\text{C}$ ,  $200^\circ\text{C}$  and  $300^\circ\text{C}$ , respectively with  $250^\circ\text{C}$  water pretreatment gave activity nearly equal to that of step-down temperature reaction test.

To investigate the effect of amount of water, the pretreatment temperature of  $250^\circ\text{C}$  was chosen. Figure 5.6 showed the effect of amount of water pretreatment of  $\text{AlPO}_4$  catalyst.

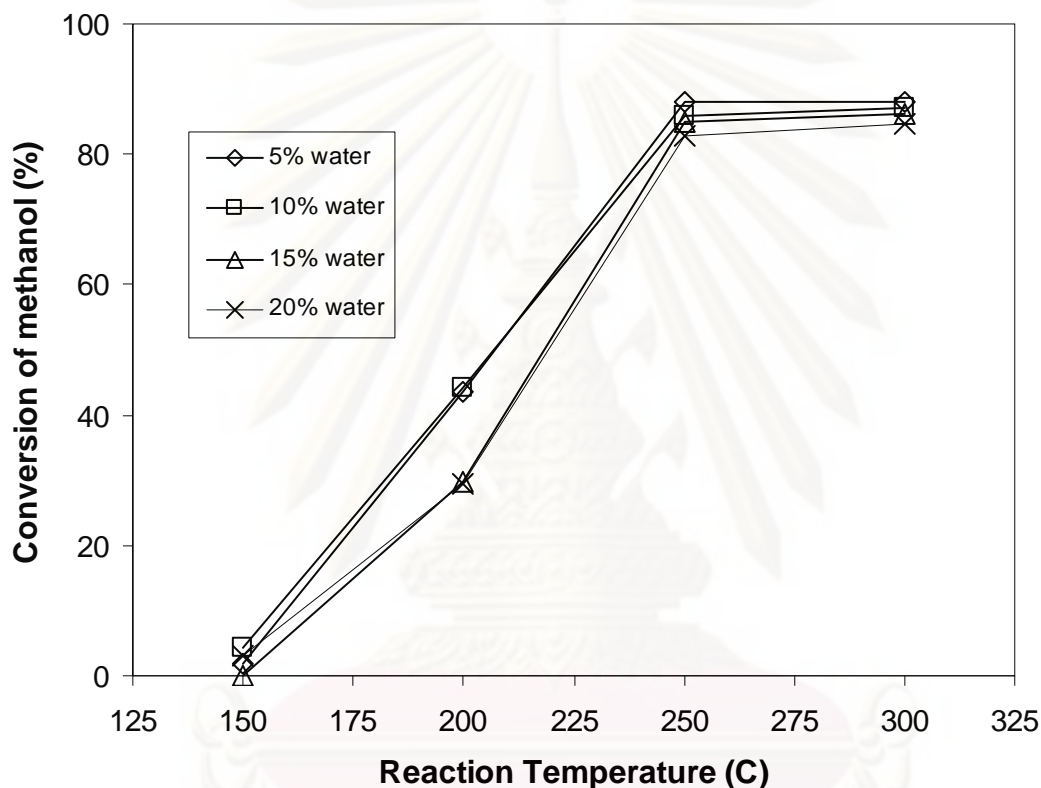


**Figure 5.6** Effect of the amount of water pretreatment of amorphous  $\text{AlPO}_4$  (0.2 g catalyst,  $\text{GHSV}=5,300 \text{ h}^{-1}$ , 10% mol water 15 minute pretreatment)

The effect of amount of water results are shown in Figure 5.6 was determined in two separated groups. Low amount of water pretreatment (5% and 10%) which gave higher methanol conversion than high amount of water pretreatment (15% and 20%), this result indicated that pretreatment  $\text{AlPO}_4$  catalyst has an appropriate range of amount of water which according to studies reported that if there is a large number of the amount water could be the poison in this reaction and caused the decreasing of activity.



In this study was aimed to investigate the effect of temperature of water pretreatment on  $\text{AlPO}_4$  catalyst more, which was continuous in section 5.3 below.

### 5.3 Characterization of treated catalysts

#### 5.3.1 Thermogravimetric analysis (TGA)

Thermogravimetric analysis or TGA is a type of testing that is performed on samples to determine changes in weight in relation to change in temperature. The results of TGA are shown in Figure 5.7. They are determined in two separated groups, fresh and  $100^\circ\text{C}$  water pretreatment  $\text{AlPO}_4$  which had more percent weight loss than the others,  $200\text{-}300^\circ\text{C}$  water pretreatment  $\text{AlPO}_4$ . This result indicated that pretreatment  $\text{AlPO}_4$  of water vapor at  $100^\circ\text{C}$  still had adsorbed water more than others. In other words, water, which is one of the reaction products, is believed to block the active sites for methanol consumption through competitive adsorption with methanol on the catalyst surface which large amount of water produced in both methanol synthesis and methanol [Xu, 1997].

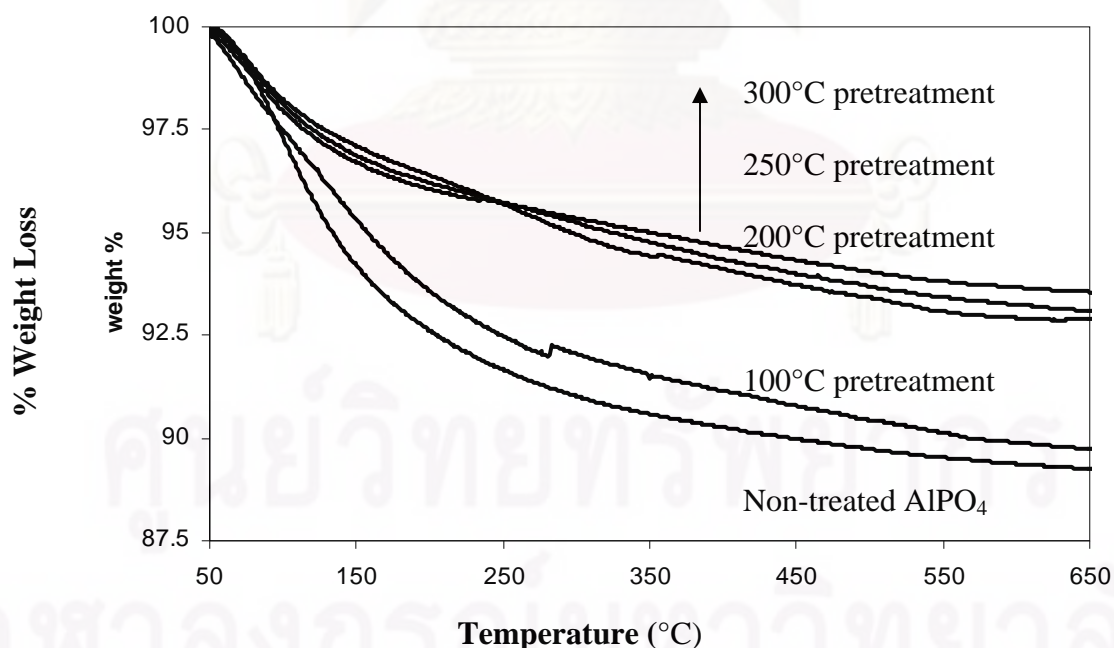


**Figure 5.7** TGA profile of treated and non-treated amorphous  $\text{AlPO}_4$  from  $50\text{-}650^\circ\text{C}$

The excess water which may be the weak bond chemisorption water could not accelerate reaction and became a poison of catalyst. According to study of Xu et al. [Xu, 1997], the presence of water in this reaction has a strong inhibiting effect on the activity of  $\gamma\text{-Al}_2\text{O}_3$ , whereas the effect is less significant over zeolite (H-ZSM-5). The partial pressure of methanol was kept constant at 81.4 Torr, and different amounts of water were added to the gas stream to determine the effect of water on catalytic activity over  $\gamma\text{-Al}_2\text{O}_3$ . The water partial pressure has a large negative effect on the catalytic activity for DME formation. With the addition of 23 Torr of water into the reagent stream, methanol conversion decreased from 17.5% to 5.8% at 188°C. Apparently, in the presence of excess water, a higher reaction temperature is required in order to achieve the same level of conversion. For example, 10% methanol conversion was attained at 180°C without the addition of water in the reagent stream; however, in the presence of 113 Torr of water, the same level of conversion was achieved at about 225°C, and only reached 39% at 250°C. (In the syngas-to-methanol process, the optimum reaction temperature is 250°C).

### 5.3.2 Fourier transform Infrared (FT-IR)

Fourier transform spectroscopy is a measurement technique whereby spectra are collected based on measurements of the coherence of a radiative source, using time-domain or space-domain measurements of the electromagnetic radiation or other type of radiation. It could be used to indicate the functional groups of material.

Adsorbed water that bonded as surface hydroxyl group (-OH) on the catalyst surface may affect acidity and activity of  $\text{AlPO}_4$ . The surface hydroxyl group of  $\text{AlPO}_4$  was investigated by FT-IR. The hydroxyl groups according to those reported by several authors could be divided into 2 major types, the hydroxyl stretching vibrations bands of adsorbed molecular water absorption (surface hydroxyls) and hydrogen-bonded of hydroxyl groups (lattice hydroxyls). FT-IR represented hydroxyl groups was separated into two regions; peak centered  $1650\text{ cm}^{-1}$  for physisorption water (surface hydroxyls) and peak around  $2500\text{-}4000\text{ cm}^{-1}$  for chemisorption water (lattice hydroxyls) [Armaroli, 2000 and Kaewgun, 2009] . Figure 5.8 showed absorption bands of treated and non-

treated  $\text{AlPO}_4$  catalyst from wavelength  $400\text{-}1800\text{ cm}^{-1}$  to investigate surface hydroxyls of catalysts.

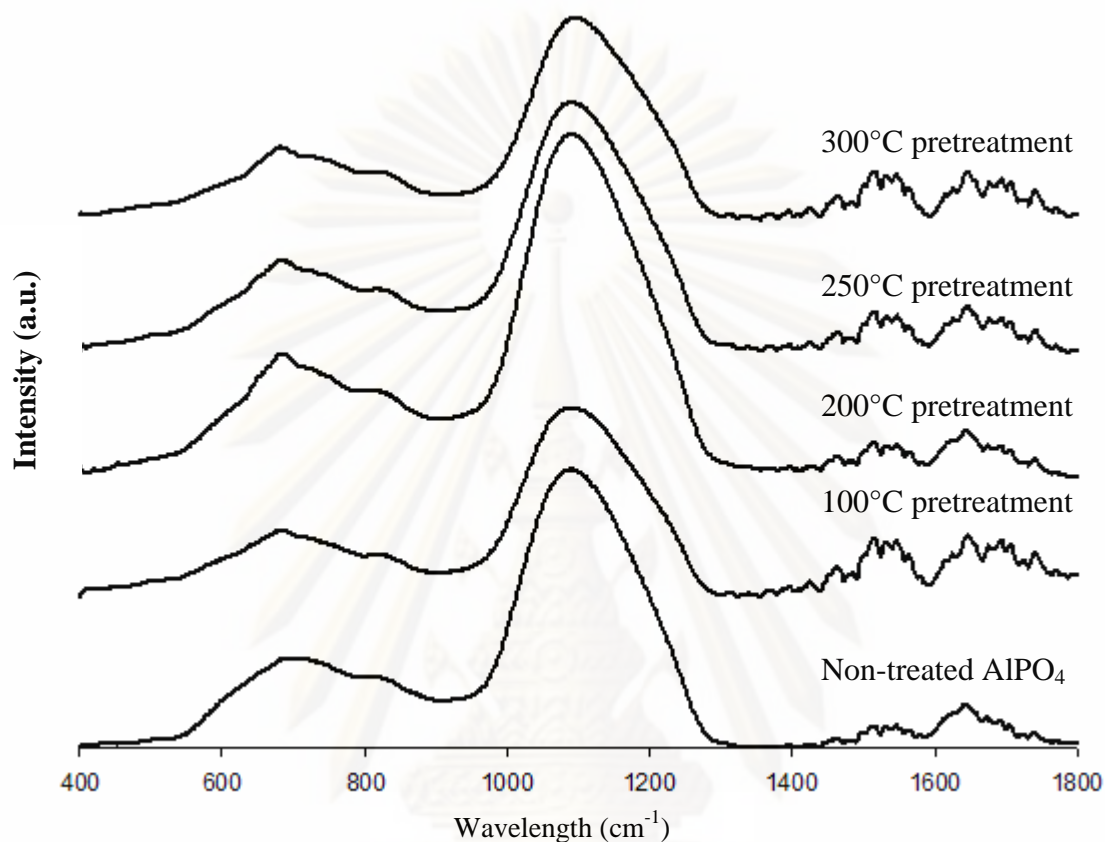


**Figure 5.8** FTIR adsorption bands from wavelength of  $400\text{-}1800\text{ cm}^{-1}$  of non-treated  $\text{AlPO}_4$  and  $100\text{-}300^\circ\text{C}$  water pretreatment  $\text{AlPO}_4$

From Figure 5.8, the regions in the range around  $400\text{-}800\text{ cm}^{-1}$  was attributed to the asymmetric and symmetric stretching frequencies of  $\text{Al-O-P}$  bonds, which correspond to non-stoichiometric aluminum phosphates [Kumar, 2006]. The peak that centered around  $1100\text{ cm}^{-1}$  was attributed to phosphate group of catalyst the vibration corresponding to phosphate group of catalyst which were attributed to the  $\text{PO}_2$  in a chain structure with two oxygen atoms from phosphorous coordination sphere bonded to aluminum atoms while the other two peaks correspond to the  $\text{P=O}$  bonds [Kumar, 2006]. These peaks that identified  $\text{Al-O-P}$  and  $\text{PO}_2$  confirmed that the catalysts were aluminum phosphate. Another peak centered around  $1650\text{ cm}^{-1}$  was assigned to the water molecules

(HOH) or surface hydroxyls of catalysts [Sun, 2007]. The results show that there were no differences of these 3 functional groups of these regions of FT-IR including surface hydroxyls or the physisorption water on the catalyst. However, the other region, lattice hydroxyls, has given different results. Figure 5.9 shows absorption bands of treated and non-treated  $\text{AlPO}_4$  catalyst from wavelength  $2500\text{--}4000\text{ cm}^{-1}$  in order to investigate lattice hydroxyls of catalysts.

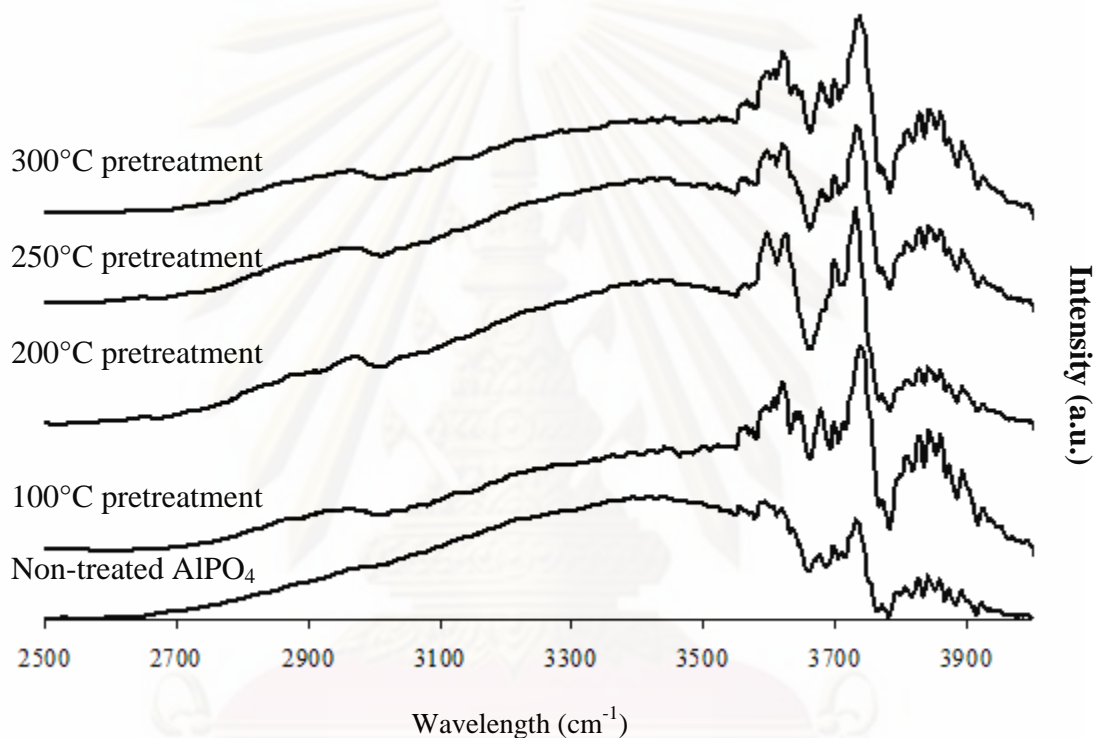


**Figure 5.9** FTIR adsorption bands from wavelength of  $2500\text{--}4000\text{ cm}^{-1}$  of non-treated  $\text{AlPO}_4$  and  $100\text{--}300^\circ\text{C}$  water pretreatment  $\text{AlPO}_4$

The hydroxyl stretching vibration of hydrogen-bonded region of wavelength of  $2500\text{--}4000\text{ cm}^{-1}$  with large broad adsorption band centered near  $3400\text{ cm}^{-1}$  could be attributed by several authors to the chemisorption of water molecule in samples according to several authors. Figure 5.9 could be separated into 5 main peaks, carried out by deconvolution of FT-IR spectra by using “fityk 0.7.4” curve fitting program (GNU General Public License, version 2, as published by the free software foundation) [Keawgun, 2008]. These regions could be attributed around wavelength of 2950, 3400, 3600, 3750 and 3800

$\text{cm}^{-1}$ , except for FT-IR peak of  $2950 \text{ cm}^{-1}$  wavelength of fresh  $\text{AlPO}_4$  catalyst that did not obviously occur. Figure 5.10-5.14 show de-convolution FT-IR spectra of each catalyst.

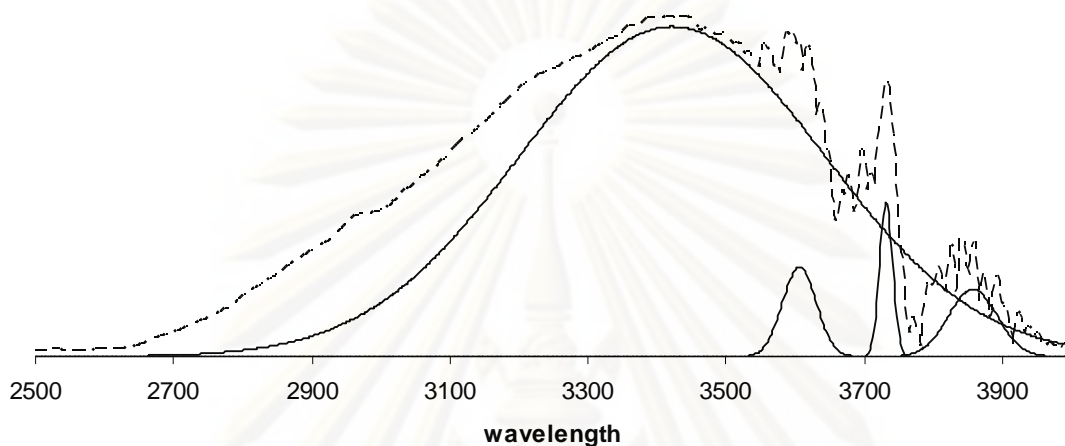


**Figure 5.10** De-convolution FT-IR spectra of hydroxyl group of non-treated  $\text{AlPO}_4$

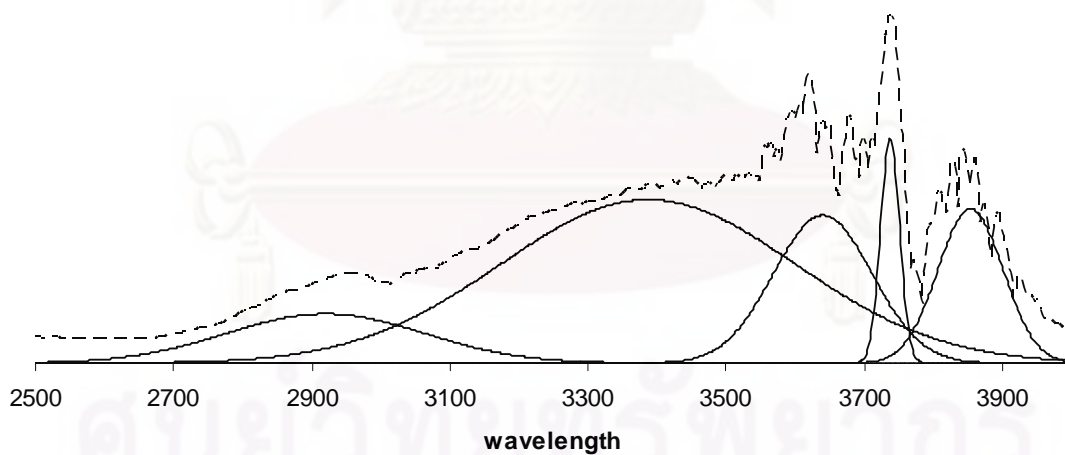


**Figure 5.11** De-convolution FT-IR spectra of hydroxyl group of water pretreatment  $100^\circ\text{C}$   $\text{AlPO}_4$ , 10% mol water for 15 minute

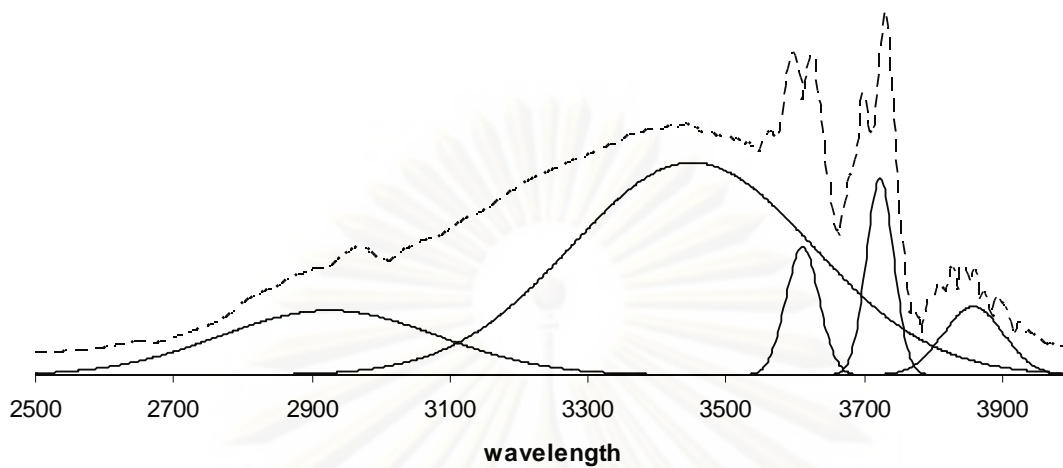


**Figure 5.12** De-convolution FT-IR spectra of hydroxyl group of water pretreatment 200°C  $\text{AlPO}_4$ , 10% mol of water for 15 minute

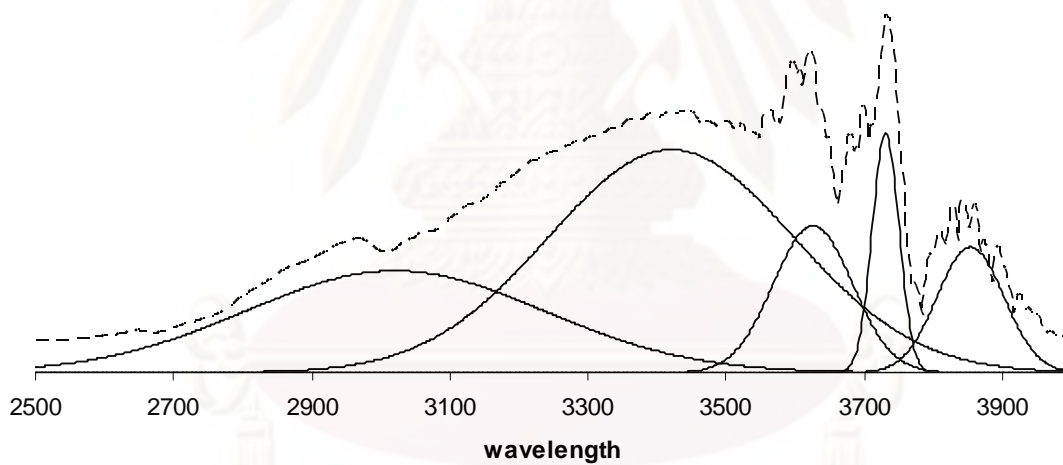


**Figure 5.13** De-convolution FT-IR spectra of hydroxyl group of water pretreatment 250°C  $\text{AlPO}_4$ , 10% mol of water for 15 minute

ศูนย์วิจัยทรัพยากร  
จุฬาลงกรณ์มหาวิทยาลัย

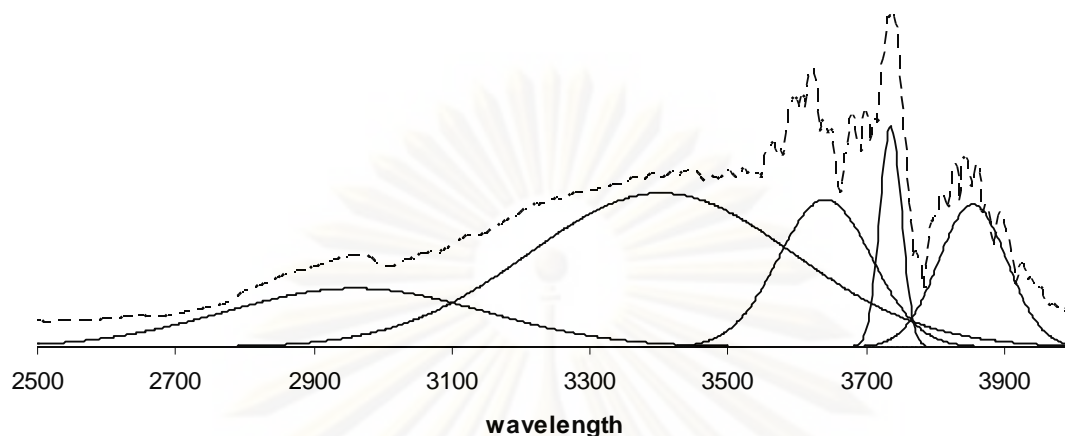


**Figure 5.14** De-convolution FT-IR spectra of hydroxyl group of 300°C water pretreatment  $\text{AlPO}_4$ , 10% mol of water for 15 minute

The results show that water pretreatment catalyst had more amount of hydroxyl group than fresh one, due to their significant higher intensity of FT-IR at wavelengths of 2950, 3600 and 3750  $\text{cm}^{-1}$ . The strong sharp band around 3750  $\text{cm}^{-1}$  which was also accompanied by a broad band around 3400  $\text{cm}^{-1}$ , could be assigned to the hydroxyl stretching mode of surface phosphate or pyrophosphate species as reported by Armaroli et al., [Sun, 2007]. The shoulders that appeared around 2900  $\text{cm}^{-1}$  of pretreatment catalysts probably indicated the presence of hydroxyl groups of various strengths attached to phosphorous in these samples [Kumar, 2006]. The results of both 2950  $\text{cm}^{-1}$  and 3750  $\text{cm}^{-1}$  band indicated that there was an increase of hydroxyl on phosphate group in catalyst after water pretreatment. In the other words, molecules of water were adsorbed and bonded with phosphorous atoms in catalyst in the form of P-OH group.

### 5.3.3 Fourier transform Raman (FT-Raman)

To investigate and confirm the result of phosphate group from FT-IR, FT-Raman spectroscopy analysis was carried out. According to phosphate Raman bands, Figure 5.15 shows Raman spectra from Raman shift of 900-1500  $\text{cm}^{-1}$  of fresh  $\text{AlPO}_4$  and 100-300°C pretreated  $\text{AlPO}_4$  catalyst. The Raman band at 1050 and 1200  $\text{cm}^{-1}$  indicate the presence

of  $\text{PO}_3^{2-}$  and  $\text{PO}_2^{1-}$  compounds, respectively [Hernandez, 2006]. Moreover, Raman study of phosphate groups by de Jager and Prinsloo indicated that Raman shift of  $876\text{--}992\text{ cm}^{-1}$  could be P-OH band in several structure, according to Raman-shift due to matrix effect and phosphate functional groups formula such as  $\text{PO}_2^{1-}$ ,  $\text{PO}_3^{2-}$ ,  $\text{PO}_4^{3-}$  and  $\text{P}_2\text{O}_7^{2-}$  [de Jager, 2001]. Raman shift of  $985\text{ cm}^{-1}$  that occurred after water pretreatment could be attributed to P-OH band and confirmed the result of FT-IR that water could adsorbed and chemical bonding with phosphate groups.

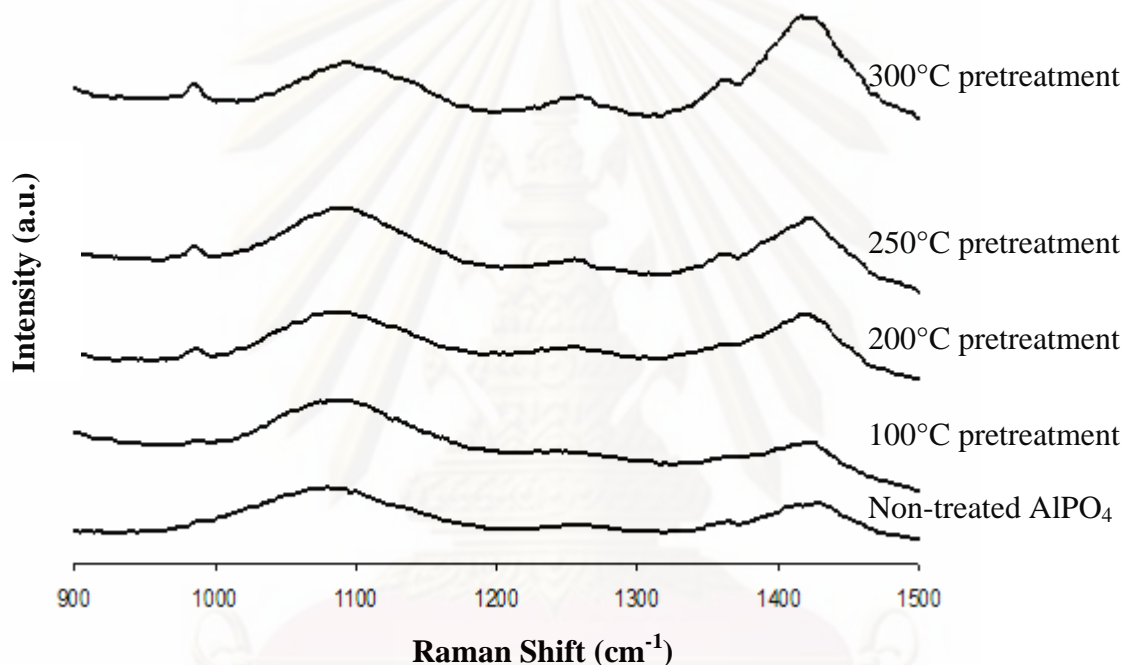
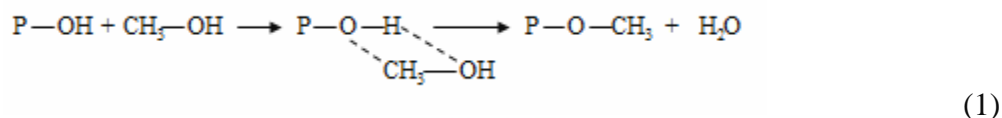


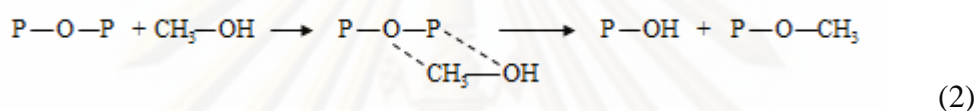
**Figure 5.15** FT-Raman spectra bands at Raman shift of  $900\text{--}1500\text{ cm}^{-1}$  of non-treated  $\text{AlPO}_4$  and  $100\text{--}300\text{ }^\circ\text{C}$  pretreatment  $\text{AlPO}_4$

The importance of existing of P-OH group was not only the proof that water could be adsorbed and changed Lewis acid site to Bronsted acid site, but also P-OH group has been reported as the initial step for methanol etherification over the orthophosphate surface obviously involves water condensation at the Bronsted acid sites and formation of methoxy groups on the surface [Cheng, 1984]. The mechanism of dehydration of methanol has been shown in reactions 1 to 4 below.

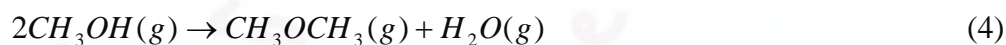
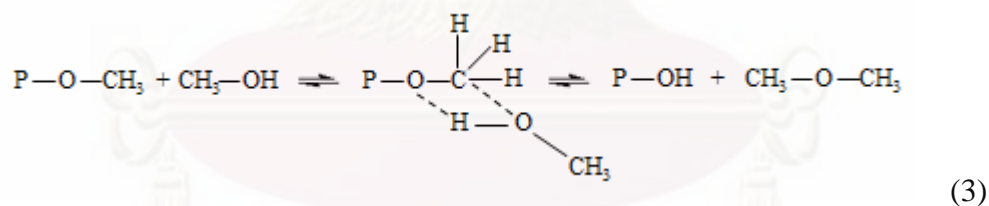




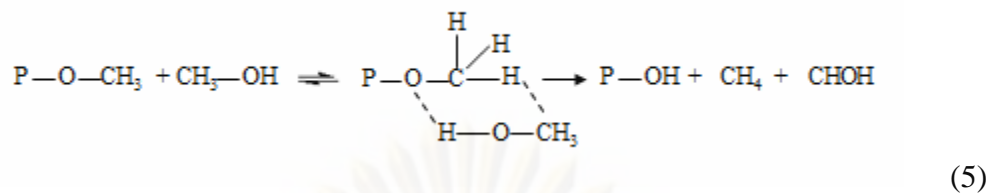
This methoxy group is considered to be high polar due to the strong electronegativity of the phosphate group. On the other hand, the breakup of P-O-P bonds resulting in the formation of methoxy groups and Bronsted acid sites probably accounts for the catalytic activities observed on pyrophosphate samples.



The methoxy species can then react with methanol through a four-member ring electron transfer process to form dimethyl ether as shown in equation 3 and summary from equation 1-3 to equation 4. This mechanism has indicated that to increase activity of amorphous  $\text{AlPO}_4$  catalyst in methanol dehydration reaction, both amount and strength of bond of P-OH group were needed.



Moreover, this process, however, is probably in competition with a six-member ring electron transfer process in equation 5 which leads to the formation of methane and formaldehyde.



The latter product is considered to be the precursor in the formation of hydrogen, carbonmonoxide and coke as shown in equation 6 and 7 evidence for process in equation 4 is that small amounts of formaldehyde and carbonmonoxide were always detected in this study.



#### 5.3.4 Catalyst active site

A number of studies indicated that methanol dehydration reaction needed appropriate acid site as active sites. The mechanism proposed by Cheng also indicated functional group of P-OH was the active site of this reaction. To investigate amount of P-OH of treated  $\text{AlPO}_4$ , the semi-quantity analysis was used by taking the ratio of interesting peak area of treated  $\text{AlPO}_4$  and reference peak of the catalyst to normalized and compared amount of P-OH. From the FT-IR result, ratio of the areas of deconvoluted hydroxyl groups peak at the wavelength of  $2950 \text{ cm}^{-1}$  and  $3750 \text{ cm}^{-1}$  and the Al-O-P at wavelength of  $833 \text{ cm}^{-1}$  and from result of FT-Raman, ratio of area of P-OH at  $985 \text{ cm}^{-1}$  and  $\text{PO}_2^{-1}$  at  $1200 \text{ cm}^{-1}$  were determined. The amount of P-OH by semi-quantity analysis from both FT-IR and FT-Raman are shown in Table 5.3.

The semi-quantity analysis of functional group of P-OH from both FT-IR and FT-Raman show that after  $250^\circ\text{C}$  pretreatment of  $\text{AlPO}_4$ , the highest amount of P-OH was obtained, which corresponded to the highest activity of such catalyst from reaction test result. The pretreatment at  $300^\circ\text{C}$  had less acidic because too high temperature pretreatment may break chemisorption bond of water resulting in give lowers activity. However, it should be noted that only amount of P-OH at wavelength of  $2950 \text{ cm}^{-1}$  from

FT-IR that followed activity trend from reaction test. To investigate and re-checked the result of semi-quantity analysis, acidity of treated and non-treated catalysts were obtained. The amine titration using Hammett indicators was selected as the acidity measurement method to investigate strength and amount of acid sites reported in range depending on acid strength ( $pK_a$ ) of indicators. In this study, methyl red, methyl orange, methyl yellow and crystal violet were employed as indicators. Distribution of the acidic strength with the amount of acid in different range of Hammett indicators is shown in Table 5.4.

**Table 5.3** Amount of P-OH group of treated  $AlPO_4$  from result of FT-IR and FT-Raman calculated by semi-quantity analysis method

Treated $AlPO_4$	FT-IR wavelength ( $cm^{-1}$ )		FT-Raman
	2950	3750	P-O-H
100°C pretreatment	0.49	0.36	0.00846
200°C pretreatment	1.23	0.16	0.02431
250°C pretreatment	1.35	0.42	0.03245
300°C pretreatment	0.91	0.41	0.02871

**Table 5.4** Distribution of the acidic strength with the amount of acid of treated and non-treated  $AlPO_4$  in different range of Hammett indicators

Catalyst	Amount of acid in range of Hammett indicators (mmol/g)			
	Methyl red	Methyl orange	Methyl yellow	Crystal violet
Non-treated $AlPO_4$	n/d	n/d	n/d	n/d
100°C pretreatment	0.266	n/d	n/d	n/d
200°C pretreatment	0.276	n/d	n/d	n/d
250°C pretreatment	0.359	n/d	n/d	n/d
300°C pretreatment	0.340	n/d	n/d	n/d

**Note** if solution colored in base form before titration, acidity cannot be determined by amine titration and was symbolic as 'n/d'

The amine titration using methyl red as Hammett indicators has shown that water pretreatment could increase strength of  $AlPO_4$  because of all treated catalysts changed

color to acid form of methyl red. However, non-treated catalyst colored in base form, which mean fresh  $\text{AlPO}_4$  had lower acid strength than methyl red of  $\text{pK}_a = 4.8$  and after water pretreatment,  $\text{AlPO}_4$  had higher acidity than  $\text{pK}_a = 4.8$ . Although, the different of acid strength of each treated  $\text{AlPO}_4$  cannot be determined due to all of suspended treated catalyst solution had color in base form when using higher strength acidity Hammett indicators which cannot be titrated by amine. The acid strength of treated  $\text{AlPO}_4$  was in the range of  $\text{pK}_a = 4.8$  to 3.7 followed acidity of methyl red and methyl orange respectively. The amount of increased acid sites from water pretreatment was determined by methyl red which water pretreatment  $250^\circ\text{C}$  gave highest amount of active site and  $100^\circ\text{C}$  pretreatment gave the lowest. Although, the amount from amine titration was not followed by the results from reaction test, the amount of acid sites from FT-Raman and amine titration were similar.

Based on characterization results, it is determined that the catalyst activity of  $\text{AlPO}_4$  could be increased by water pretreatment because of formation of P-OH group and increasing of both strength and amount of acid site on the surface of catalyst. The appropriate temperature of water pretreatment with 10% mol water in GHSV of  $5300 \text{ h}^{-1}$  flow rate for 15 minute was  $200\text{-}250^\circ\text{C}$ , which gave the best performance of activity of  $\text{AlPO}_4$  in methanol dehydration reaction.

## CHAPTER VI

### CONCLUSIONS AND RECOMMENDATIONS

#### 6.1 Conclusions

The activity of catalysts in methanol dehydration were ordered by amorphous  $\text{AlPO}_4$ , solvothermal  $\gamma\text{-Al}_2\text{O}_3$ , and commercial  $\gamma\text{-Al}_2\text{O}_3$  respectively, which were followed their amount of acidity and surface area as determined from  $\text{NH}_3$ -TPD and  $\text{N}_2$  adsorption. Both  $\gamma\text{-Al}_2\text{O}_3$  and  $\text{AlPO}_4$  catalysts showed increasing of activity when temperature direction during reaction test changed from step-up to step-down. The activity increasing was suggested being the presence of water product during dehydration reaction. The effect of water pretreatment on  $\text{AlPO}_4$  catalyst was then investigated under various pretreatment temperature conditions.

From FT-IR and FT-Raman results, it is determined that the catalyst activity of  $\text{AlPO}_4$  could be increased by water pretreatment because of formation of P-OH group. Amine titration also showed increasing of both strength and amount of acid site on the surface of catalyst. The appropriate temperature of water pretreatment with 10% mol water in GHSV of  $5300\text{ h}^{-1}$  flow rate for 15 minute was  $200\text{-}250^\circ\text{C}$ , which gave the best performance of activity of  $\text{AlPO}_4$  in methanol dehydration reaction.

In addition, the presence of water at  $100^\circ\text{C}$  pretreatment became  $\text{AlPO}_4$  poison which indicated by TGA and FT-Raman that physisorbed water could block the adsorption of methanol on catalyst active sites instead.

#### 6.2 Recommendations

From this experiment, we have expected to improve acidity of catalyst for syngas production. Recommendations for the future work are the following:

1. To determine type of acidity (Bronsted and Lewis) with Fourier Transform Infrared Spectrophotometer (FTIR) or proton solid-state Nuclear magnetic resonance ( $^1\text{H}$  MAS NMR spectra) for amorphous  $\text{AlPO}_4$ , solvothermal  $\gamma\text{-Al}_2\text{O}_3$ , and

commercial  $\gamma\text{-Al}_2\text{O}_3$  catalysts to determine phenomenon that Lewis acid sites could be changed to Brønsted acid sites and which have stronger acidity.

2. The appropriate water pretreatment condition i.e. temperature and amount of water of  $\gamma\text{-Al}_2\text{O}_3$  may difference.



ศูนย์วิจัยทรัพยากร  
จุฬาลงกรณ์มหาวิทยาลัย

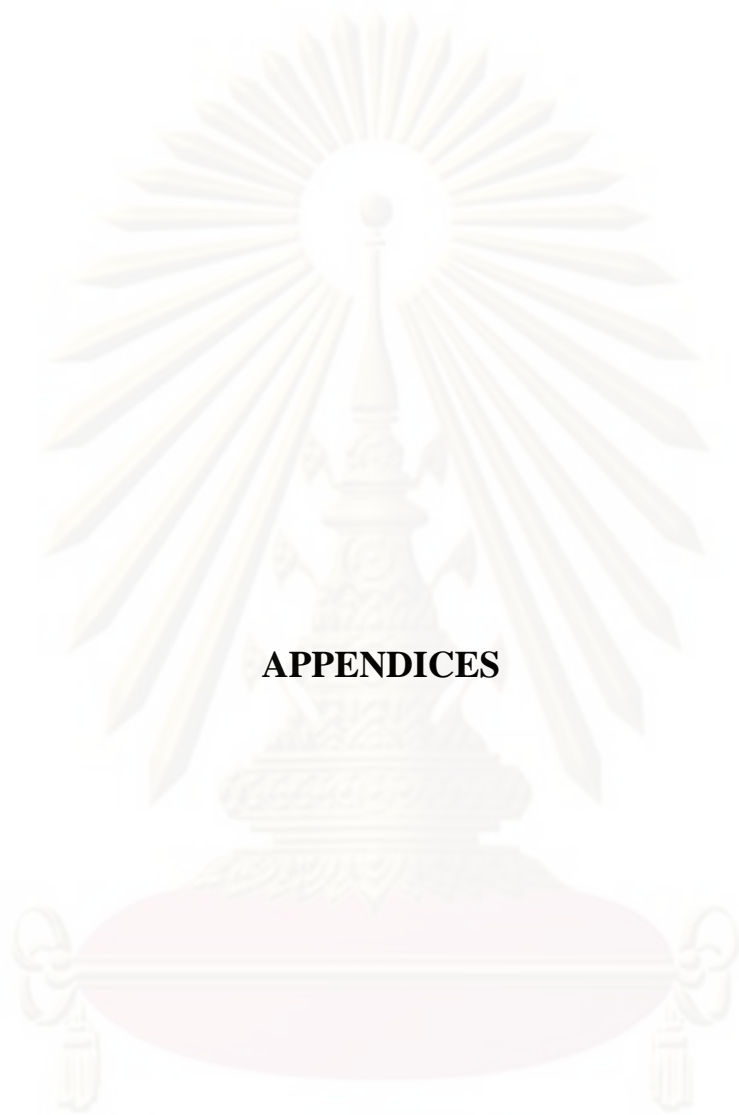
## REFERENCES

- Armaroli, T., Trombetta, M., Alejandre, A. G., Solis, J. R. and Busca, G. FTIR study of the interaction of some branched aliphatic molecules with the external and internal sites of H-ZSM5 zeolite. Physical Chemistry Chemical Physics 2 (2000): 3341-3348
- Bautista, F. M., Campelo, J. M., Garcia, A., Luna, D., Marinas, J. M., Quiros, R. A. and Romero, A. A. Influence of acid-base properties of catalysts in the gas-phase dehydration-dehydrogenation of cyclohexanol on amorphous AlPO<sub>4</sub> and several inorganic solids. Applied Catalysis a-General 243 (2003): 93-107
- Chatterjee, A. A reactivity index study to rationalize the effect of dopants on Bronsted and Lewis acidity occurring in MeAlPOs. Journal of Molecular Graphics & Modelling 24 (2006): 262-270
- Cheng, S. Decomposition of Alcohols over Zirconium and Titanium Phosphate. Ind. Eng. Chem. Prod. Res. Dev. 23 (1984): 219-225
- de Jager, H. J. and Prinsloo, L. C. The dehydration of phosphates monitored by DSC/TGA and in situ Raman spectroscopy. Thermochimica Acta 376 (2001): 187-196
- Fei, J. H., Hou, Z. Y., Zhu, B., Lou, H. and Zheng, X. M. Synthesis of dimethyl ether (DME) on modified HY zeolite and modified HY zeolite-supported Cu-Mn-Zn catalysts. Applied Catalysis a-General 304 (2006): 49-54
- Fu, Y. C., Hong, T., Chen, J. P., Auroux, A. and Shen, J. Y. Surface acidity and the dehydration of methanol to dimethyl ether. Thermochimica Acta 434 (2005): 22-26
- Hernandez, M., Genesca, J., Uruchurtu, J., Galliano, F. and Landolt, D. Effect of an inhibitive pigment zinc-aluminum-phosphate (ZAP) on the corrosion mechanisms of steel in waterborne coatings. Progress in Organic Coatings 56 (2006): 199-206
- Jun, K. W., Lee, H. S., Roh, H. S. and Park, S. E. Catalytic dehydration of methanol to dimethyl ether (DME) over solid-acid catalysts. Bulletin of the Korean Chemical Society 23 (2002): 803-806

- Kaewgun, S., Nolph, C. A., Lee, B. I. and Wang, L. Q. Influence of hydroxyl contents on photocatalytic activities of polymorphic titania nanoparticles. Materials Chemistry and Physics 114 (2009): 439-445
- Khom-In, J., Praserttham, P., Panpranot, J. and Mekasuwandumrong, O. Dehydration of methanol to dimethyl ether over nanocrystalline Al<sub>2</sub>O<sub>3</sub> with mixed gamma- and chi-crystalline phases. Catalysis Communications 9 (2008): 1955-1958
- Kim, S. D., Baek, S. C., Lee, Y. J., Jun, K. W., Kim, M. J. and Yoo, I. S. Effect of gamma-alumina content on catalytic performance of modified ZSM-5 for dehydration of crude methanol to dimethyl ether. Applied Catalysis a-General 309 (2006): 139-143
- Kumar, V. S., Padmasri, A. H., Satyanarayana, C. V. V., Reddy, I. A. K., Raju, B. D. and Rao, K. S. R. Nature and mode of addition of phosphate precursor in the synthesis of aluminum phosphate and its influence on methanol dehydration to dimethyl ether. Catalysis Communications 7 (2006): 745-751
- Ludmany, A., Kurek, S. S., Stoklosa, A., Wilczynski, G., Wojtowicz, A. and Zajecki, J. Amorphous titanium hydrogenphosphate - an inorganic sorbent and a catalyst. Applied Catalysis a-General 267 (2004): 149-156
- Qi, L., Lee, B. I., Badheka, P., Wang, L. Q., Gilmour, P., Samuels, W. D. and Exarhos, G. J. Low-temperature paraelectric-ferroelectric phase transformation in hydrothermal BaTiO<sub>3</sub> particles. Materials Letters 59 (2005): 2794-2798
- Ramos, F. S., de Farias, A. M. D., Borges, L. E. P., Monteiro, J. L., Fraga, M. A., Sousa-Aguiar, E. F. and Appel, L. G. Role of dehydration catalyst acid properties on one-step DME synthesis over physical mixtures. Catalysis Today 101 (2005): 39-44
- Semelsberger, T. A., Borup, R. L. and Greene, H. L. Dimethyl ether (DME) as an alternative fuel. Journal of Power Sources 156 (2006): 497-511
- Vishwanathan, V., Jun, K. W., Kim, J. W. and Roh, H. S. Vapour phase dehydration of crude methanol to dimethyl ether over Na-modified H-ZSM-5 catalysts. Applied Catalysis a-General 276 (2004): 251-255



- Vishwanathan, V., Roh, H. S., Kim, J. W. and Jun, K. W. Surface properties and catalytic activity of TiO<sub>2</sub>-ZrO<sub>2</sub> mixed oxides in dehydration of methanol to dimethyl ether. Catalysis Letters 96 (2004): 23-28
- Xu, M. T., Lunsford, J. H., Goodman, D. W. and Bhattacharyya, A. Synthesis of dimethyl ether (DME) from methanol over solid-acid catalysts. Applied Catalysis a-General 149 (1997): 289-301
- Yaripour, F., Baghaei, F., Schmidt, I. and Perregaard, J. Synthesis of dimethyl ether from methanol over aluminium phosphate and silica-titania catalysts. Catalysis Communications 6 (2005): 542-549
- Yaripour, F., Baghaei, F., Schmidt, I. and Perregaard, J. Catalytic dehydration of methanol to dimethyl ether (DME) over solid-acid catalysts. Catalysis Communications 6 (2005): 147-152
- Yurdakoc, M., Akcay, M., Tonbul, Y. and Yurdakoc, K. Acidity of silica-alumina catalysts by amine titration using Hammett indicators and FT-IR study of pyridine adsorption. Turkish Journal of Chemistry 23 (1999): 319-327



**APPENDICES**

ศูนย์วิทยทรัพยากร  
จุฬาลงกรณ์มหาวิทยาลัย

## APPENDIX A

### CALCULATIONS OF METHANOL AND WATER FLOW RATE AND TEMPERATURE CONDITION

#### 1. Methanol concentration

from Antoine's equation

$$\ln P = A - \frac{B}{(T + C)} \quad (1)$$

Define: P = vapor pressure (mmHg)  
A, B, C = constant value  
T = temperature, (K)

Constant value of methanol for calculation vapor pressure

$$A = 7.89750 \quad B = 1474.08 \quad C = 229.13$$

For methanol, substitute in Antoine's equation

$$\ln P = 7.8975 - \frac{1474.08}{((273.15 + 29) + 229.13)}$$

$$\ln P = 5.1286$$

$$P = 168.7807 \text{ mmHg}$$

$$\begin{aligned} \text{Pressure from tank} &= 16.25 \text{ psig} \\ &= 840.136 \text{ mmHg} \end{aligned}$$

$$\begin{aligned} \text{Volume of methanol} &= 168.7807/840.136 \\ &= 20.09 \% \end{aligned}$$

#### 2. Water concentration

Constant value of methanol for calculation vapor pressure

Using different Antoine's equation

$$\log_{10} P = A - \frac{B}{(T + C)} \quad (2)$$

Define: P = vapor pressure (mmHg)  
A, B, C = constant value

T = temperature, (°C)

Constant value of methanol for calculation vapor pressure

Temperature from 0°C to 60°C

A = 8.10765            B = 1750.286            C = 235

Temperature up from 60°C to 100°C

A = 7.96681            B = 1668.21            C = 228

Then to calculate in percent mol concentration, define

$$\%mol = \frac{P_{sat}(water)}{P(system)} \quad (3)$$

System pressure is atmospheric pressure = 760 mmHg

Calculation using equation (2) and (3)

5% mol of water vapour, control temperature is 33°C

10% mol of water vapour, control temperature is 47°C

15% mol of water vapour, control temperature is 54°C

20% mol of water vapour, control temperature is 61°C

ศูนย์วิทยทรัพยากร

จุฬาลงกรณ์มหาวิทยาลัย

## APPENDIX B

### CALIBRATION CURVES

This appendix shows the calibration curves for calculation of composition of products in reforming reaction of methane by carbon dioxide over supported nickel catalysts. The main product of reforming reaction of methane is carbon monoxide, carbon dioxide, hydrogen and methane.

The Thermal Conductivity Detector (TCD), gas chromatography Shimadzu model 8AIT was used to analyze the concentration of product by using Porapak-Q and Porapak-N column.

Mole of reagent in y-axis and area reported by gas chromatography in x-axis are exhibited in the curves. The calibration curves of carbon monoxide, carbon dioxide, hydrogen and methane are illustrated in Figure B1-B7, respectively.

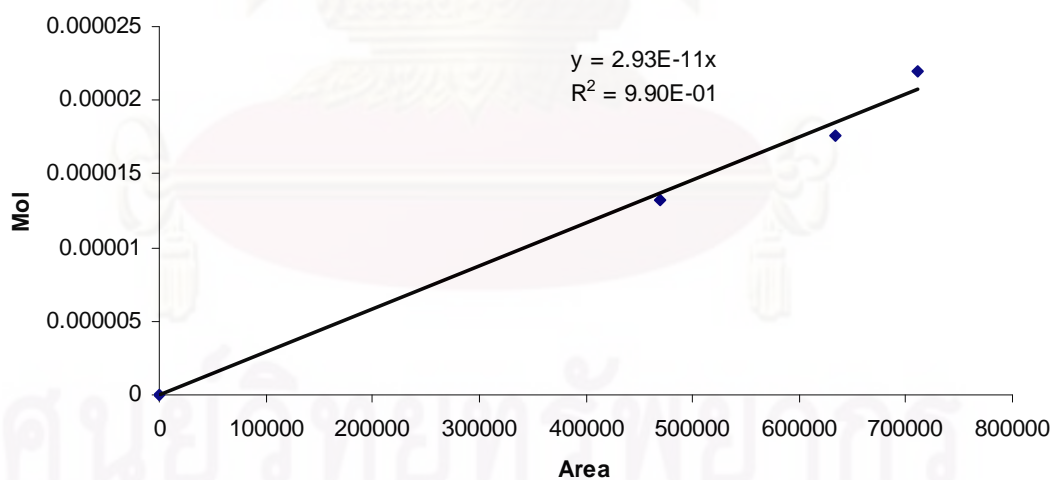


**Figure B1** The calibration curve of methanol from Porapak-Q.

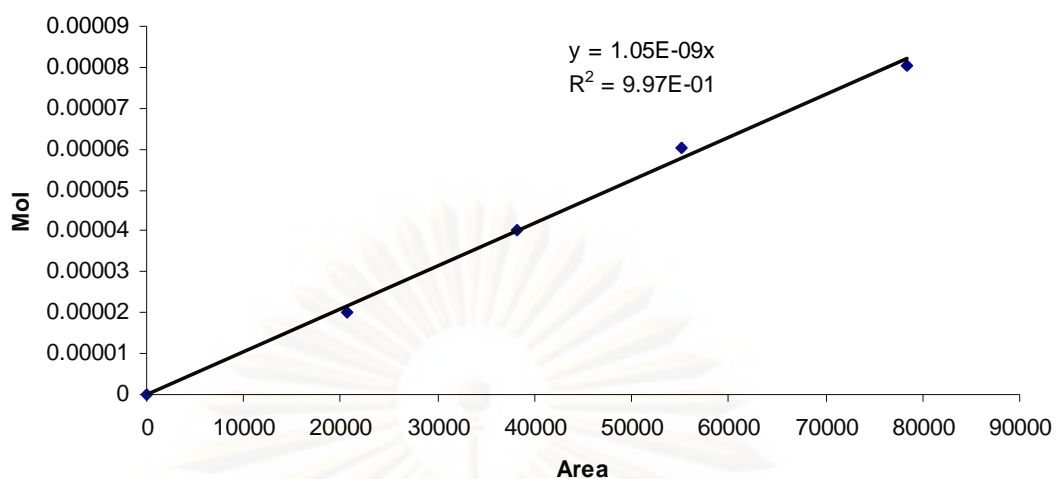


**Figure B2** The calibration curve of water from Porapak-Q.

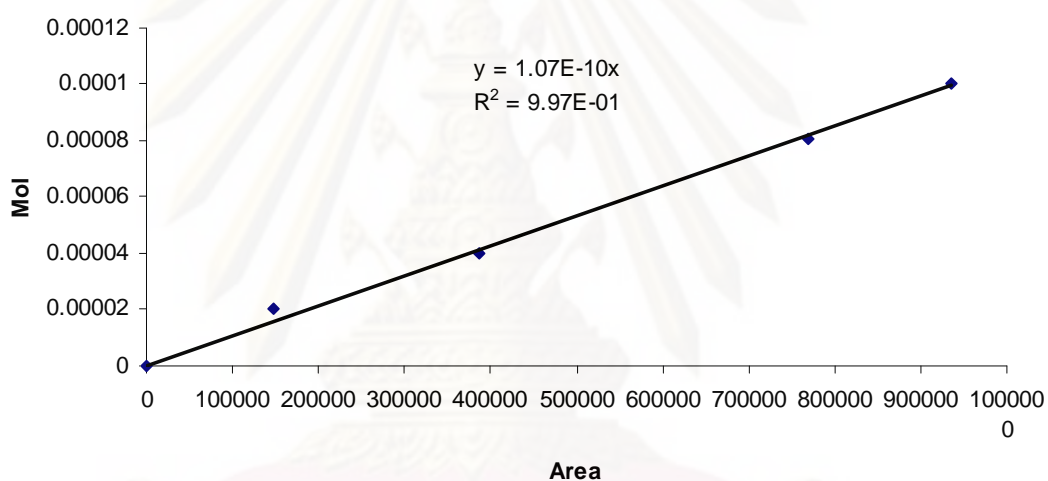


**Figure B3** The calibration curve of DME from Porapak-Q.

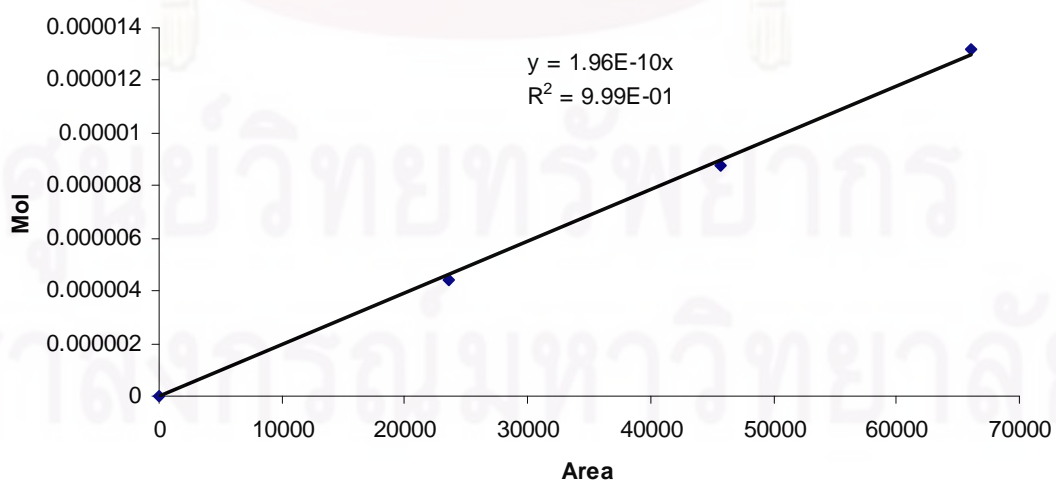


**Figure B4** The calibration curve of methanol from Porapak-N.

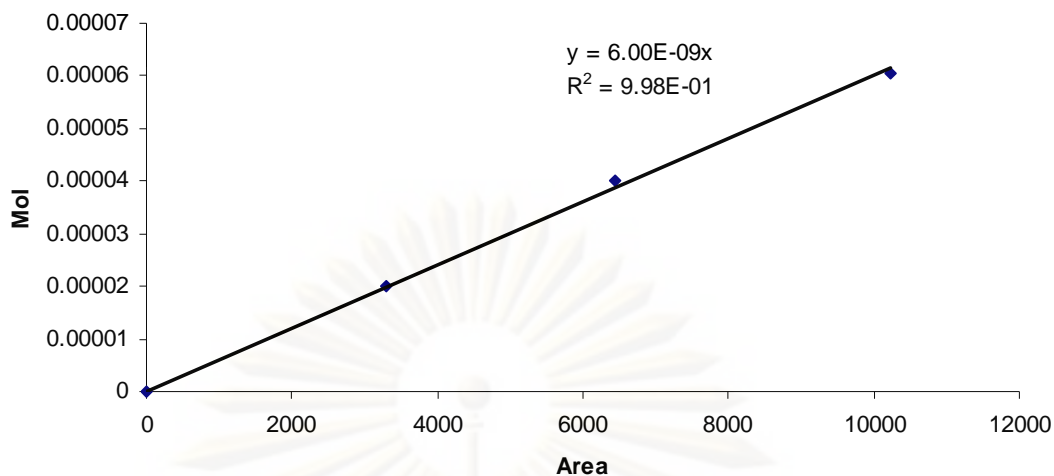


**Figure B5** The calibration curve of water from Porapak-N.

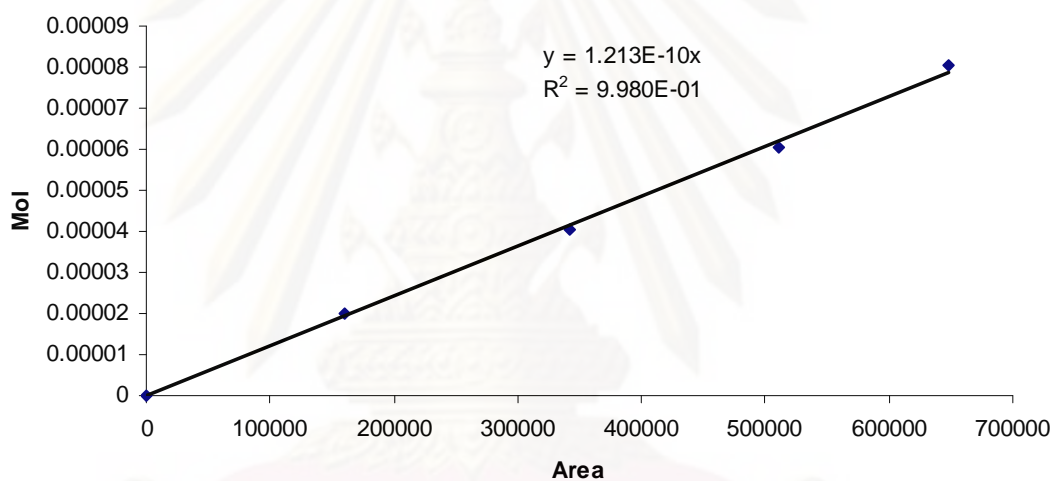


**Figure B6** The calibration curve of water from Porapak-N.

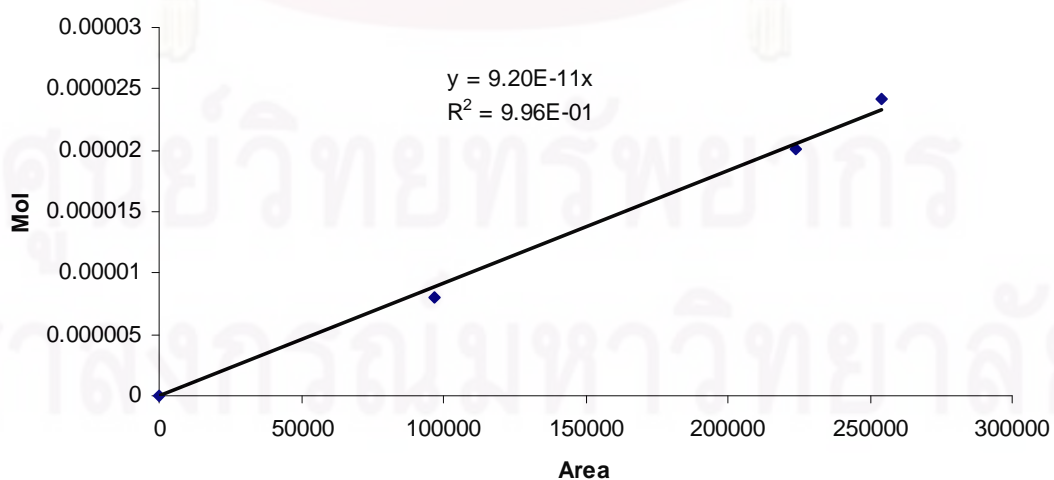


**Figure B7** The calibration curve of carbon monoxide from Porapak-N.

## APPENDIX C

### DATA OF CALCULATION OF ACID SITE

#### Calculation of total acid sites

For example, TS-1 sample, total acid site is calculated from the following step.

#### 1. Conversion of total peak area to peak volume

Conversion from Micromeritics Chemisorb 2750 is equal to 77.5016 ml/area unit. Therefore, total peak volume is derived from

Example: commercial gamma alumina catalyst give total peak area is 2.134 area

$$\begin{aligned}\text{Total peak volume} &= 77.5016 \times \text{total peak area} \\ &= 77.5016 \times 2.134 \\ &= 165.388 \text{ ml}\end{aligned}$$

#### 2. Calculation for adsorbed volume of 15% NH<sub>3</sub>

$$\begin{aligned}\text{Adsorbed volume of 15\% NH}_3 &= 0.15 \times \text{total peak volume} \\ &= 0.15 \times 165.388 \text{ ml} \\ &= 24.80 \text{ ml}\end{aligned}$$

#### 3. Total acid sites are calculated from the following equation

$$\text{Total acid sites} = \frac{(\text{Adsorbed volume, ml}) \times 101.325 \text{ Pa}}{\left(8.314 \times 10^{-3} \frac{\text{Pa} \cdot \text{ml}}{\text{K} \cdot \mu\text{mol}}\right) \times 298 \text{ K} \times (\text{weight of catalyst, g})}$$

For commercial gamma alumina catalyst sample, 0.1001 g of this sample was measured, therefore



$$\begin{aligned} \text{Total acid sites} &= \frac{24.80 \text{ ml} \times 101.325 \text{ Pa}}{\left(8.314 \times 10^{-3} \frac{\text{Pa} \cdot \text{ml}}{\text{K} \cdot \mu\text{mol}}\right) \times 298 \text{ K} \times (0.1001 \text{ g})} \\ &= 10.14 \text{ mmol H}^+/\text{g}. \end{aligned}$$



ศูนย์วิจัยทรัพยากร  
จุฬาลงกรณ์มหาวิทยาลัย

## APPENDIX D

### LIST OF PUBLICATION

Krit Lertjiamratn, Joongjai panpranot, “Effect of water pretreatment on alumina-based catalysts in methanol dehydration”, Proceeding of the 19<sup>th</sup> Thailand Chemical Engineering and Applied Chemical Conference, Kanchanaburi, Thailand, Oct. 25-27, 2009



ศูนย์วิจัยทรัพยากร  
จุฬาลงกรณ์มหาวิทยาลัย

## VITA

Mr. Krit Lertjiamratn was born on June 24<sup>th</sup>, 1985 in Bangkok, Thailand. He finished high school from Suankularb wittayalai School in 2003, and received the bachelor's degree of Chemical Engineering (Second Class Honors) from Faculty of Engineer, King Mongkut's Institute of Technology Ladkrabang in April 2007. He continued her master's study at Department of Chemical Engineering, Faculty of Engineering, Chulalongkorn University in June, 2007.



ศูนย์วิทยทรัพยากร  
จุฬาลงกรณ์มหาวิทยาลัย